

Radial velocity measurements of Subdwarf B stars

C.M. Copperwheat¹, L. Morales-Rueda², T.R. Marsh¹,
P.F.L. Maxted³ and U. Heber⁴

¹ *Department of Physics, University of Warwick, Coventry, CV4 7AL, UK*

² *Symetrica Security Ltd., Phi House, Southampton Science Park, Southampton, SO16 7NS, UK*

³ *Astrophysics Group, Keele University, Keele, Staffordshire, ST5 5BG, UK*

⁴ *Dr. Reimis-Sternwarte, Astronomisches Institut der Universität Erlangen-Nürnberg, Sternwartstr. 7, 96049 Bamberg, Germany*

Received:

ABSTRACT

Subdwarf B (sdB) stars are hot, sub-luminous stars which are thought to be core-helium burning with thin hydrogen envelopes. The mechanism by which these stars lose their envelopes has been controversial but it has been argued that binary star interaction is the main cause. Over the past decade we have conducted a radial velocity study of a large sample of sdB stars, and have shown that a significant fraction of the field sdB population exists in binary systems. In 2002 and 2003 we published 23 new binary sdB stars and the definitions of their orbits. Here we present the continuation of this project. We give the binary parameters for 28 systems, 18 of which are new. We present also our radial velocity measurements of a further 108 sdBs. Of these, 88 show no significant evidence of orbital motion. The remaining 20 do show radial velocity variations, and so are good candidates for further study. Based on these results, our best estimate for the binary fraction in the sdB population is 46 – 56 per cent. This is a lower bound since the radial velocity variations of very long period systems would be difficult to detect over the baseline of our programme, and for some sources we have only a small number of measurements.

Key words: binaries: close — binaries: spectroscopic — subdwarfs

1 INTRODUCTION

Subdwarf B stars (sdBs) are hot ($T_{\text{eff}} = 25,000 - 40,000$ K), core helium-burning stars with masses $\sim 0.5M_{\odot}$ and thin hydrogen envelopes of mass $\leq 0.02M_{\odot}$ (Heber et al. 1984; Saffer et al. 1994, see also Heber 2009 for a recent review). D’Cruz et al. (1996) proposed that such a star could form if a red giant star with a degenerate helium core were to lose its envelope when it is within ~ 0.4 mag of the tip of the red giant branch (RGB). In this scenario, the core could go on to ignite helium despite the mass loss. This model explains the masses of sdB stars as a consequence of the core mass at the helium flash.

The loss of the hydrogen envelope could be due to an enhancement of the stellar wind, or binary interactions. It has been shown that a large fraction of sdB stars are now members of short period binary systems (Maxted et al. 2001; Napiwotzki et al. 2004). Close binary systems such as these imply a ‘common envelope’ phase, which occurs due to dynamically unstable transfer when the more massive star reaches the red giant phase of its evolution. Orbital energy is then lost to friction, resulting in a shortening of the bi-

nary period (Iben & Livio 1993). The common envelope is eventually ejected, leading to an sdB primary star with a close main sequence or white dwarf companion (Han et al. 2002, 2003). Yungelson & Tutukov (2005) argued that all sdB stars come from binaries, with the apparently single examples either the product of merging pairs of helium white dwarfs or members of long-period systems which have avoided the common envelope phase (Green et al. 2001), and whose radial velocity variations we have yet to detect.

SdB stars are of interest because they are a strong test of population synthesis models, since they are much less influenced by the selection effects which compromise other close binary populations, such as cataclysmic variables (Pretorius et al. 2007). They are also an ideal population for testing models of the common envelope phase, and sdBs with massive white dwarf companions are one of the potential progenitors for type Ia supernovae (Tutukov & Yungelson 1981; Webbink 1984).

Following the detection of many close binary sdBs by Maxted et al. (2001), we began a project with the aim of measuring the orbits of a large number of binary systems. In Maxted et al. (2002) and Morales-Rueda et al. (2003) we

published the parameters of 23 systems. We present here the continuation of this study.

2 OBSERVATIONS AND REDUCTION

A complete journal of our observations is given in Table 1. The number of radial velocity observations which we list in this table are those which are presented in this paper, in addition to the measurements previously presented in Maxted et al. (2002) and Morales-Rueda et al. (2003).

The majority of the data used in this study were collected using the Intermediate Dispersion Spectrograph (IDS) mounted on the 2.5m Isaac Newton Telescope. Our earliest observations in 2000/2001 used the 500mm camera with the R1200R grating centred on H α and the TEK (1k \times 1k) CCD giving a dispersion of 0.37 $\text{\AA}/\text{pix}$ and a resolution of 0.9 \AA . Subsequent observations used the 235 mm camera with the R1200B grating and the thinned EEV10 (2k \times 4k) CCD, giving a dispersion of 0.48 $\text{\AA}/\text{pix}$ and a resolution of 1.4 \AA . The central wavelength used with this grating varied slightly between observing runs, but in all cases was chosen to cover H β and H γ . In 2003 we expanded this project to cover southern targets with the first of a series of observing runs using the grating spectrograph plus the SITE CCD mounted on the 1.9 m telescope at the Sutherland site of the South African Astronomical Observatory (SAAO). Grating 4, with 1200 grooves per mm, was used to obtain spectra covering H γ and H β with a dispersion of 0.5 $\text{\AA}/\text{pix}$ and a resolution of better than 1 \AA at 4600 \AA .

We took two consecutive observations of each object and bracketed them with CuAr frames to calibrate the spectra in wavelength. After debiasing and flatfielding the frames (using Tungsten flatfield frames for the INT/IDS observations and dome flats for the SAAO observations), spectral extraction proceeded according to the optimal algorithm of Marsh (1989). The arcs were extracted using the profile associated with their corresponding target to avoid systematic errors caused by the spectra being tilted. Uncertainties on every point were propagated through every stage of the data reduction.

3 RESULTS

3.1 Radial velocity measurements

To measure the radial velocities we use least squares fitting of a model line profile and follow the same procedure described in Morales-Rueda et al. (2003). The model line profile consists of three Gaussians with different widths and depths. For any given sdB, the widths and depths of the Gaussians are optimised and then fixed while their velocity offsets from the rest wavelengths of the lines in question are fitted separately for each spectrum; see Maxted et al. (2000) for further details of this procedure. For the red spectra obtained in Apr 2000 - May 2001 we fit the H α line. For all other spectra the fitting was performed simultaneously for H β and H γ .

In Tables 9 and 10 we list all of our radial velocity measurements. Table 9 contains the measurements for 28 systems which we have found to be binary, and for which we have found the orbital period. The description of the orbital

period determination is given in Section 3.2. Table 10 contains measurements for all of the remaining sdBs covered by our project which we have not previously published, a total of 108 objects. Most of these objects show no evidence for orbital variations, and so are likely to be either single sdBs, or binary systems in which the mass function is too low for us to detect radial velocity variations (due to a low companion mass, a long binary period, a binary inclination close to zero or a combination of these factors). For some objects the non-detection of variation may be because the number of observations of that object is small. In some other cases, there are clear signs that the sdB is in a binary system, however there are still competing orbital aliases of comparable significance and so our data is insufficient to determine the true orbital period. These are strong candidates for future observation. In this paper we will concentrate on the 28 solved systems given in Table 9. In Section 4.3 we discuss the binary fraction of the sdB population and in Section 4.4 we investigate the nature of the companion stars. For these sections we consider the complete list of objects in our programme.

3.2 Determination of orbital periods

In radial velocity work, while one can very soon determine a star to be binary, it can take much longer to determine the orbital period. With a small amount of data there is a danger of picking an incorrect alias. This period can be very wrong, even when the quoted uncertainty is tiny, because the statistics are not Gaussian and so an error of 100 or even 1000 times the quoted uncertainty can happen. On the other hand, the process of collecting sufficient data to determine the true period beyond doubt can be very inefficient in terms of telescope time. It was therefore necessary for us to select a criterion by which we consider a binary orbit to be solved.

Our initial ‘rule of thumb’ was to consider the period in a system to be determined if the lowest minimum of the χ^2 function has a χ^2 at least 10 less than the next lowest minimum. From a Bayesian point of view, this $\Delta\chi^2 > 10$ criterion is equivalent to requiring that the second best period is $\gtrsim \exp 5 = 150$ times less probable than the best. This argument, although true, is not precise because while the peak of the second alias may be > 150 times less probable than the peak of the best alias, there is no guarantee that the total probability of *any* other period is as low. We therefore instead chose to determine the probabilities of the true orbital period being within a certain range of our favoured value. The details of this Bayesian calculation are given in Morales-Rueda et al. (2003) and Marsh et al. (1995). For the purposes of comparing the observed sdB binary period distribution to theoretical evolutionary models, knowing the orbital period to within ± 5 per cent is sufficient. We therefore established the following criterion: we considered a system to be solved if the probability that the true orbital period lies further than 5 per cent from our best alias is less than 0.1 per cent.

For 28 of our targets we have enough radial velocity measurements to satisfy this criterion. We have previously announced nine of these in conference proceedings (PG0934+186, PG1230+052, PG1244+113, PG1519+640, PG1528+104, KPD2040+3955, Morales-Rueda et al. 2003; EC00404-4429, EC02200-2338, Morales-Rueda et al. 2005,

Table 1. Journal of observations.

Dates	# of RV observations	Setup
10 – 21 Apr 2000	18	INT + IDS + 500 mm + R1200R + λ_c =H α
8 – 13 Mar 2001	72	INT + IDS + 500 mm + R1200R + λ_c =H α
1 – 8 May 2001	104	INT + IDS + 500 mm + R1200R + λ_c =H α
6 – 11 Aug 2001	76	INT + IDS + 500 mm + R1200B + λ_c =4350Å
27 Sept – 6 Oct 2001	135	INT + IDS + 500 mm + R1200B + λ_c =4350Å
27 Mar – 1 Apr 2002	175	INT + IDS + 500 mm + R1200B + λ_c =4350Å
23 – 30 Apr 2002	217	INT + IDS + 500 mm + R1200B + λ_c =4350Å
21 – 22 Mar 2003	35	SAAO 1.9m + grating spectrograph + grating #4 + λ_c =4600Å
9 – 18 Apr 2003	101	INT + IDS + 500 mm + R1200B + λ_c =4400Å
10 – 15 Sep 2003	136	SAAO 1.9m + grating spectrograph + grating #4 + λ_c =4600Å
30 Mar – 7 Apr 2004	75	SAAO 1.9m + grating spectrograph + grating #4 + λ_c =4600Å
22 – 25 Oct 2004	107	SAAO 1.9m + grating spectrograph + grating #4 + λ_c =4600Å
22 – 27 June 2005	101	SAAO 1.9m + grating spectrograph + grating #4 + λ_c =4600Å
11 – 24 Oct 2005	223	SAAO 1.9m + grating spectrograph + grating #4 + λ_c =4600Å
25 Mar – 6 Apr 2007	243	INT + IDS + 500 mm + R1200B + λ_c =4500Å
17 – 25 Aug 2007	150	INT + IDS + 500 mm + R1200B + λ_c =4500Å
18 – 27 Mar 2008	61	INT + IDS + 500 mm + R1200B + λ_c =4500Å
10 – 16 Mar 2009	82	INT + IDS + 500 mm + R1200B + λ_c =4500Å
30 Apr – 1 May 2009	12	WHT + ISIS + R600B (λ_c =4350Å) + R1200R (λ_c =H α)

EC12408-1427 Morales-Rueda et al. 2006), but we present here the more detailed analysis. The orbit of one of our targets has been independently determined (PG1000+408, Shimanskii et al. 2008) and so we present our results to corroborate this determination. The remaining 18 orbital determinations are new.

We follow the procedure described in Morales-Rueda et al. (2003), using the ‘floating mean’ periodogram (e.g. Cumming et al. 1999), which consists in fitting the data with a model composed of a sinusoid plus a constant of the form:

$$V = \gamma + K \sin(2\pi f(t - t_0)),$$

where f is the frequency ($f = 1/\text{period}$) and t is the observation time. We obtain the χ^2 of the fits as a function of frequency and select the minima of this χ^2 function. By fitting the systemic velocity, γ , at the same time as K and t_0 , we correct a failing of the Lomb-Scargle (Lomb 1976; Scargle 1982) periodogram which starts by subtracting the mean of the data and then fits a plain sinusoid. The floating mean periodogram works better than the Lomb-Scargle periodogram for small numbers of points. We obtain the χ^2 of the fit as a function of f and then identify minima in this function.

In Table 2 we give the orbital parameters for each sdB binary. listing T_0 , the systemic velocity, γ , the radial velocity semi-amplitude, K , and the reduced χ^2 achieved for the best alias. We also give the period of an N th alias, and the difference in χ^2 between this alias and the best alias. In most cases we list the $N = 2$ nd alias, and find a significant χ^2 difference between these best and second-best aliases. However, for some systems (PG0958-073, PG1000+408, PG1230+052, PG1403+316, PG1648+536, KPD2215+5037 and PG2331+038) we find that the best alias is surrounded by many other aliases which are very close in period and with a similar χ^2 . In some sense these systems are not solved since these close aliases are as significant as the best alias, but they are sufficiently close and span a sufficiently small range that our criterion is satisfied. For the purposes of Ta-

ble 2 when the nearest competing aliases are so close in period it makes more sense to compare with the next *group* of aliases, so for these systems we choose to give the N th alias for which the period differs by more than 5 per cent from the best alias. In all cases this results in a significant difference in χ^2 between this alias and the best alias.

The results of folding the radial velocities of each object on its orbital period are plotted in Figure 1. The error bars on the radial velocity points are, in most cases, smaller than the size of the symbol used to display them.

The periodograms (χ^2 versus orbital frequency) for the 28 objects listed in Table 2 are given in Figures 2 and 3. Each panel includes a blow-up of the region in frequency where the minimum χ^2 is found. It is clear from these figures that in the majority of cases there is a significant difference in χ^2 between the best and the second alias. Exceptions are the seven systems we have previously discussed in which there are many aliases close in frequency and significance to the best alias. The blow-ups illustrate that the frequency range covered by these alternate aliases is very small, so we can determine the period to within 5 per cent of the true value with confidence. Two other systems we wish to highlight are PG1452+198 and EC22202-1834. In Table 2 we compared the first and second aliases for these systems, which are very similar in significance. The periodograms for each of these two systems show that the two aliases are discrete and separate without the continuous range of intermediate aliases which we see in the previously discussed seven systems. For each system, either one of these two solutions could represent the ‘true’ period, and the χ^2 difference is too small to favour one over the other. However, in both cases the period difference between the two aliases is very small and our criterion for solution is satisfied no matter which we believe to be the true period. We therefore include these systems with those we consider to be solved.

In Table 3 we list for each system the probability that the true orbital period lies further than 1 and 5 per cent from our favoured value, using the Bayesian calculation detailed in Morales-Rueda et al. (2003) and Marsh et al. (1995). We

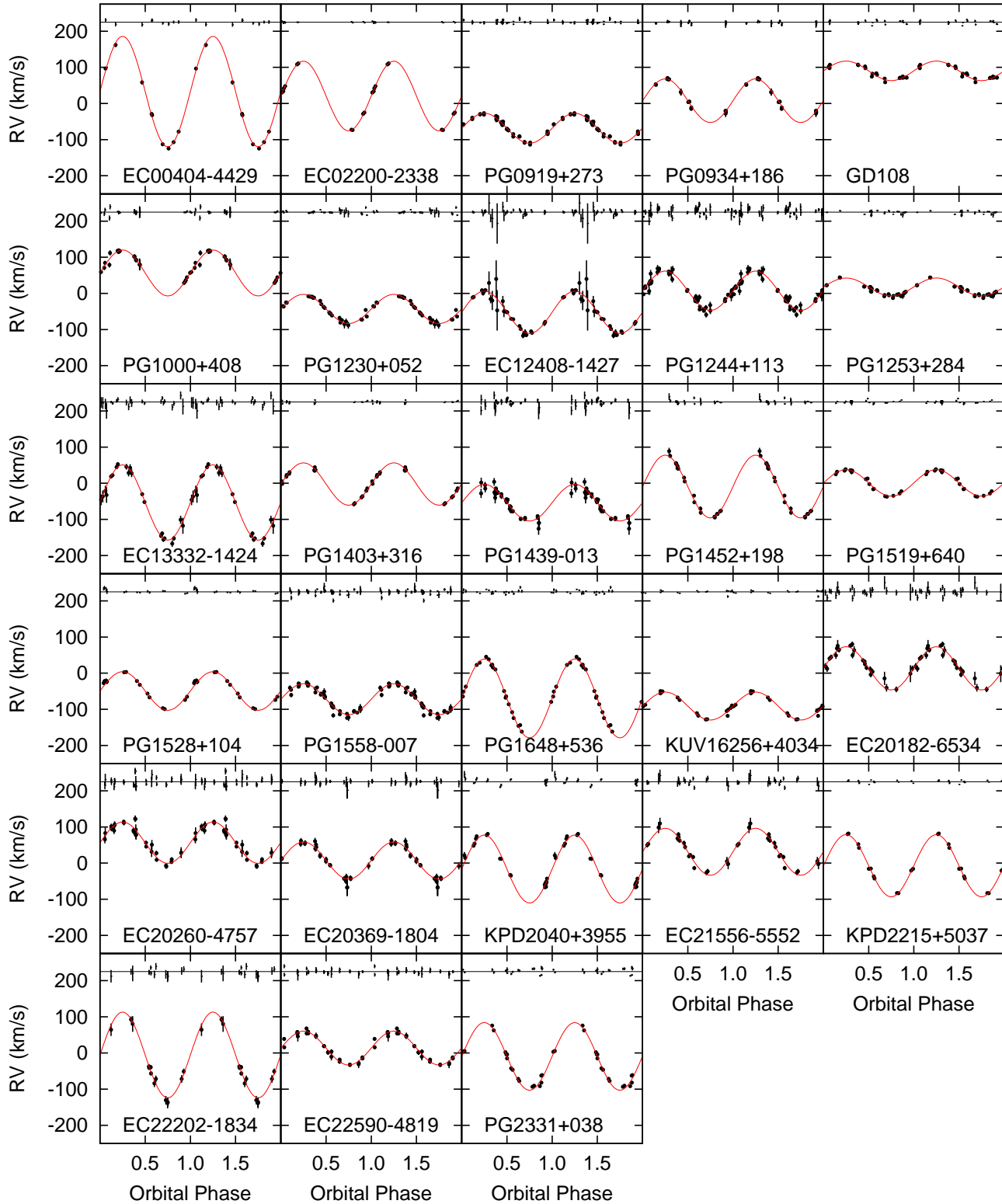


Figure 1. The radial velocity curve for each object using the parameters for the best alias give in Table 2, folded on the orbital period. For each object we also plot the residuals to the fit on the same scale, offset by 220km/s.

Table 2. List of the orbital periods measured for the 28 sdBs studied. We give T_0 , the systemic velocity, γ , the radial velocity semi-amplitude, K , and the reduced χ^2 achieved for the best alias. We also list the period of the N th best alias and the χ^2 difference between the primary and N th aliases. For the majority of targets we list the second best alias, however in the few cases where there are many aliases close in period to the primary alias, we give the first alias for which the period differs from the primary alias by ± 5 per cent. The number of data points used to calculate the orbital period is given in the final column under n .

Object	HMJD (T_0)	Period (d)	γ (km/s)	K (km/s)	$\chi^2_{reduced}$	N	N th best alias (d)	$\Delta\chi^2$	n
EC00404-4429	52894.9418(4)	0.12834(4)	33.0 ± 2.9	152.8 ± 3.4	0.82	2	0.11350(3)	74	9
EC02200-2338	52895.529(4)	0.8022(7)	20.7 ± 2.3	96.4 ± 1.4	0.27	2	0.3038(1)	61	10
PG0919+273	53274.29(4)	15.5830(5)	-68.6 ± 0.6	41.5 ± 0.8	1.23	2	14.9400(5)	43	47
PG0934+186	52376.08(1)	4.05(1)	7.7 ± 3.2	60.3 ± 2.4	0.74	2	3.59(1)	22	18
PG0958-073	53635.03(2)	3.18095(7)	90.5 ± 0.8	27.6 ± 1.4	2.31	7	2.92145(5)	29	21
PG1000+408	52920.208(7)	1.049343(5)	56.6 ± 3.4	63.5 ± 3.0	0.73	123	0.705291(2)	55	20
PG1230+052	53276.431(3)	0.837177(3)	-43.1 ± 0.7	40.4 ± 1.2	1.28	70	0.737931(2)	229	29
EC12408-1427	52954.467(5)	0.90243(1)	-52.2 ± 1.2	58.6 ± 1.5	0.72	2	9.493(1)	38	29
PG1244+113	53301.61(2)	5.75211(9)	7.4 ± 0.8	54.4 ± 1.4	1.94	2	5.8456(1)	206	51
PG1253+284	53673.77(1)	3.01634(5)	17.8 ± 0.6	24.8 ± 0.9	1.83	2	2.95692(6)	28	32
EC13332-1424	52954.418(3)	0.82794(1)	-53.2 ± 1.8	104.1 ± 3.0	0.77	2	0.455168(3)	33	22
PG1403+316	53293.779(6)	1.73846(1)	-2.1 ± 0.9	58.5 ± 1.8	0.88	28	1.63874(1)	34	16
PG1439-013	53629.87(7)	7.2914(5)	-53.7 ± 1.6	50.7 ± 1.5	1.52	2	7.1452(5)	16	38
PG1452+198	52262.240(4)	0.96498(4)	-9.1 ± 2.1	86.8 ± 1.9	0.99	2	0.97213(4)	2	20
PG1519+640	52391.389(3)	0.539(3)	0.9 ± 0.8	36.7 ± 1.2	1.29	2	0.338(2)	68	18
PG1528+104	52394.553(2)	0.331(1)	-49.3 ± 1.0	53.3 ± 1.6	1.03	2	0.491(2)	33	14
PG1558-007	53280.25(4)	10.3495(6)	-71.9 ± 0.7	42.8 ± 0.8	1.77	2	1.103666(8)	102	42
PG1648+536	53650.8209(9)	0.6109107(4)	-69.9 ± 0.9	109.0 ± 1.3	1.63	37	0.5500470(5)	202	61
KUV16256+4034	52392.498(2)	0.4776(8)	-90.9 ± 0.9	38.7 ± 1.2	1.68	2	0.958(2)	64	18
EC20182-6534	53276.834(3)	0.598819(6)	13.5 ± 1.9	59.7 ± 3.2	0.84	2	0.585875(6)	40	25
EC20260-4757	53279.37(6)	8.952(2)	56.5 ± 1.6	57.1 ± 1.9	2.25	2	0.88375(2)	22	29
EC20369-1804	53279.29(3)	4.5095(4)	7.2 ± 1.6	51.5 ± 2.3	0.57	2	0.81668(1)	20	24
KPD2040+3955	53259.232(3)	1.482860(4)	-16.4 ± 1.0	94.0 ± 1.5	3.21	2	1.494224(4)	37	20
EC21556-5552	53660.604(5)	0.8340(7)	31.4 ± 2.0	65.0 ± 3.4	1.14	2	0.4545(2)	52	18
KPD2215+5037	53258.172(2)	0.809146(2)	-7.2 ± 1.0	86.0 ± 1.5	2.04	147	0.768551(1)	103	12
EC22202-1834	53605.762(4)	0.70471(5)	-5.5 ± 3.9	118.6 ± 5.8	0.77	2	0.70884(5)	5	14
EC22590-4819	53278.25(6)	10.359(2)	13.5 ± 1.1	46.8 ± 1.8	0.84	2	0.90970(2)	46	26
PG2331+038	53234.865(3)	1.204964(3)	-9.5 ± 1.1	93.5 ± 1.9	2.68	51	0.020232962(1)	282	18

consider a period to be robust when the probability is below 0.1 per cent (or -3 in the log scale). This is not fulfilled to within 1 per cent of our favoured period for 7 of our 28 sources. The worst example is PG1519+640: for this system the probability that the true period is more than 1 per cent different from our favoured value is -0.98 in the log scale, or greater than 10 per cent. However, all of the periods are robust to within 5 per cent of our favoured values, and as we noted earlier this is the criterion by which we consider a system to be solved, since for the practical purpose of comparing the population of sdB stars to theoretical models knowing the periods to within 5 per cent is normally sufficient. In a number of cases the probability of the orbital period being further than 1 and 5 per cent from our favoured value is the same. This is because all the significant probability lies within a very small range around the best period, with all the significant competition (i.e. next best alias) placed outside the 5 per cent region around the best alias.

We also compute the uncertainty that when added in quadrature to our raw error estimates gives a reduced $\chi^2 = 1$. This systematic uncertainty accounts for sources of errors such as true variability of the star or slit-filling errors. These errors are most probably not correlated with the orbit or the statistical errors determined and thus are added in quadrature. In all cases we use a minimum value of 2 km s^{-1} corresponding to $1/10^{\text{th}}$ of a pixel which we believe

to be a fair estimate of the true limits of our data. These determinations are also given in Table 3. In most cases, the systematic uncertainty does not exceed the minimum value.

4 DISCUSSION

4.1 Effective temperature, surface gravity and helium abundance

We measured the effective temperature, T_{eff} , the surface gravity, $\log g$, and the helium abundance, $\log(\text{He}/\text{H})$, for 13 of the 28 sdBs listed in Table 2, and list these measurements in Table 4. Due to the various instrument setups we used we are not able to do this for all the systems, because data in which the spectral range only encompasses a small number of lines is insufficient to constrain these parameters with any precision. We used the procedure of Saffer et al. (1994) to fit the profiles of the Balmer, the He I and the He II lines present in the spectra by a grid of synthetic spectra. The synthetic spectra obtained from the metal line-blanketed LTE model atmospheres of Heber et al. (2000) were matched to the data simultaneously. For the two hottest stars the model grid with enhanced metal line blanketing was used, which substantially improved the fits (for details see O'Toole & Heber 2006). Before the fitting was carried out, we convolved the synthetic spectra with a Gaussian function to account for the

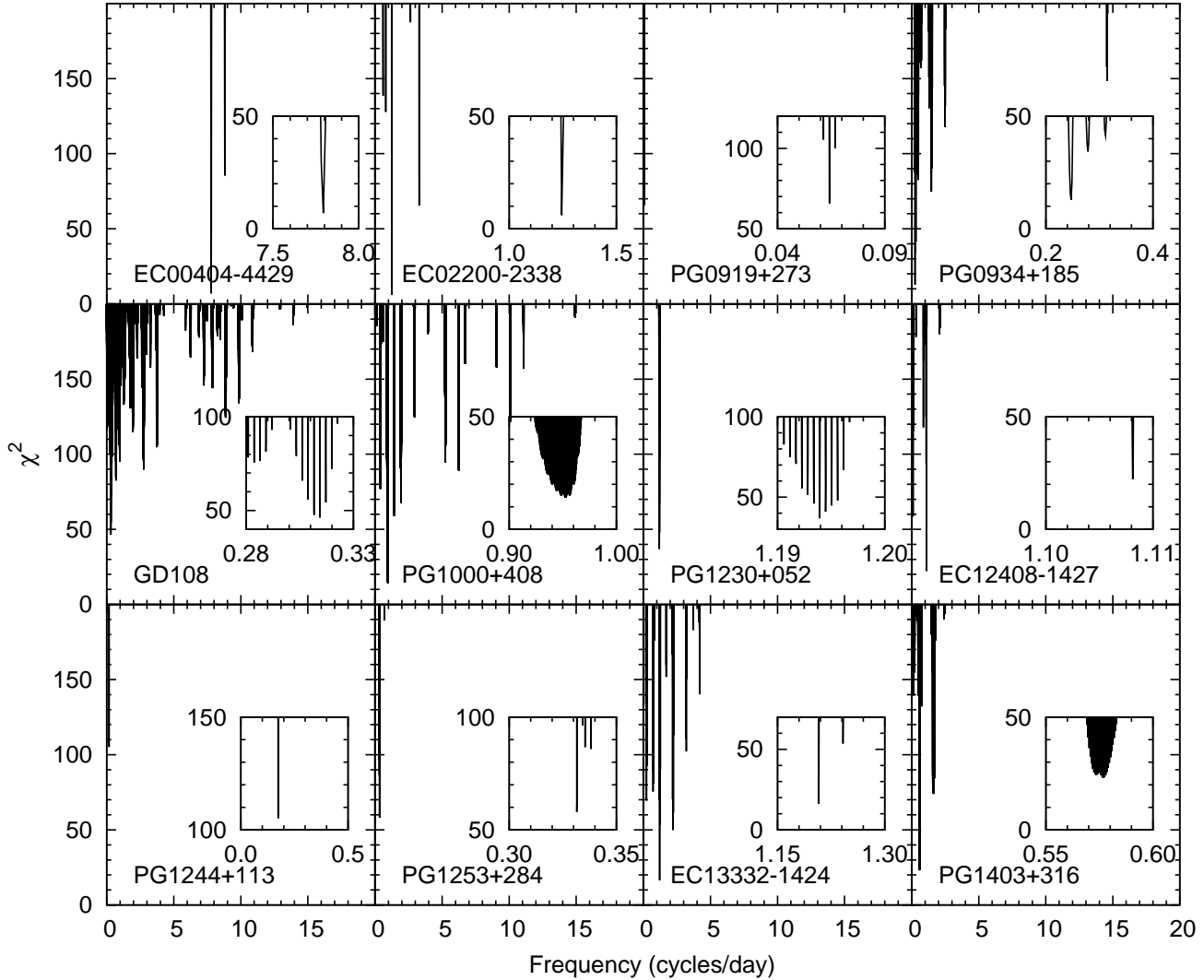


Figure 2. Periodograms for the first 12 objects listed in Table 2. Each panel presents χ^2 versus cycles/day obtained after the period search was carried out. The frequency with the smallest χ^2 corresponds to the orbital frequency of the system. For clarity we include an insert showing a blow-up of the region around the orbital frequency.

instrumental profile. KPD2215+5037 was previously analysed with the same set of models in Heber et al. (2002), the results of which are in exact agreement with our finding here.

We plot these results in the $T_{\text{eff}} / \log g$ plane and find that all but two of the objects lie in the band defined by the zero-age extreme horizontal branch, the terminal-age extreme horizontal branch and the He main sequence (Figure 2 of Maxted et al. 2001) and are therefore extreme horizontal branch (EHB) stars. The two exceptions are the two hottest stars, PG0934+186 and PG1244+113, which are sufficiently displaced from the band to be considered post-EHB stars. The effective temperature and gravity of PG1244+113 were determined by Saffer (as reported by Maxted et al. 2001) with a method similar to ours but using a different grid of synthetic spectra to be $T_{\text{eff}} = 33800\text{K}$ and $\log g = 5.67$, which places it just outside of the EHB band, although the uncertainty on the measurement was such that it could not

be positively identified as a post-EHB star. We determine a somewhat higher T_{eff} and lower gravity, which places the star away from the EHB.

We also note that we find EC22133-6446 to be one of the rare helium-rich sdB stars. EC22133-6446 is one of the objects in our survey in which we detect no significant radial velocity variations.

4.2 Orbital ellipticity

Edelmann et al. (2005) took high-resolution spectra of 15 sdB binaries, and for a third of these found the orbits to be slightly eccentric with $e \sim 0.03 - 0.06$. To investigate ellipticity in our binaries we fitted each of our data sets using the Levenburg-Marquardt method (Press 2002) with a model consisting of a sine function and its first harmonic, a reasonable approximation to an elliptical orbit for small

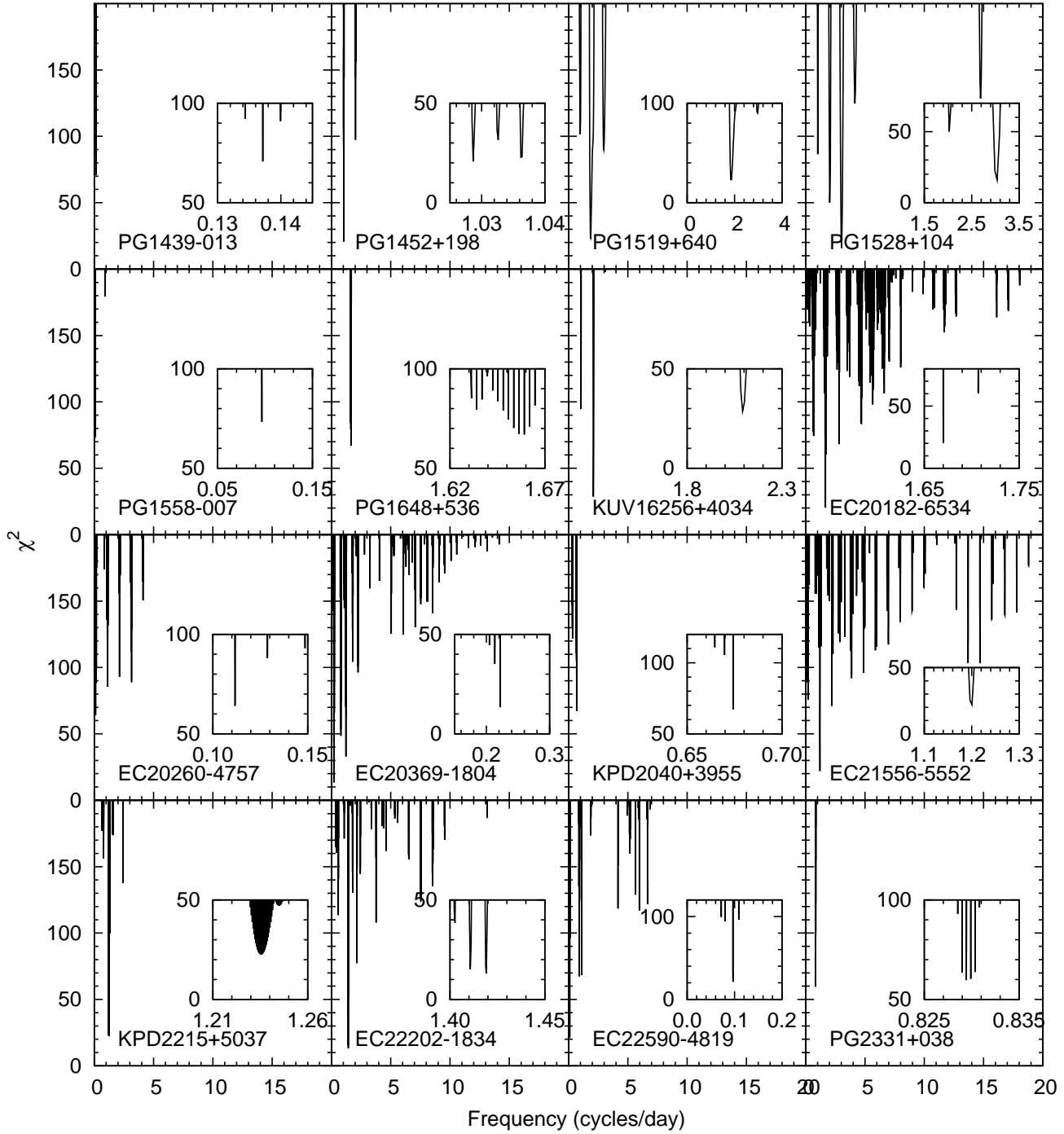


Figure 3. Periodograms as in Figure 2 for the remaining 16 objects listed in Table 2.

values of e . The eccentricity is determined from the ratio of the amplitudes of the first harmonic to the fundamental. In Table 5 we list the best-fit value of e for each target, and the improvement in χ^2 over a circular orbit. The change in the orbital period determination compared to the values reported in Table 2 is very small (less than one per cent in all cases, and much less than this in most). For each target, we computed the F statistic comparing the elliptical model fit

with the circular fit. In all cases, we find the improvement is not significant at the 95% level. We therefore find that there is no evidence of ellipticity in any of our radial velocity curves, not even at long periods where departures from circular orbits might be expected.

One important caveat is that our observations were not designed to detect ellipticity in these systems, and it is unlikely that our lower-resolution observations were capable of

Table 3. List of probabilities that the true orbital period of a system lies further than 1 and 5 per cent from our favoured value given in Table 2. Numbers quoted are the logs in base 10 of the probabilities. Column number 4 gives the value of the systematic uncertainty that has been added in quadrature to the raw error to give a χ^2 that lies above the 2.5 per cent probability in the χ^2 distribution.

Object	1%	5%	systematic error (km s ⁻¹)
EC00404-4429	-15.09	-15.09	2
EC02200-2338	-11.35	-11.35	2
PG0919+273	-9.26	-37.27	2
PG0934+186	-3.14	-4.62	2
PG0958-073	-1.42	-3.35	3
PG1000+408	-1.37	-9.57	2
PG1230+052	-17.23	-49.72	2
EC12408-1427	-7.54	-7.54	2
PG1244+113	-25.47	-27.97	4
PG1253+284	-2.70	-14.94	3
EC13332-1424	-5.69	-7.33	2
PG1403+316	-5.06	-5.94	2
PG1439-013	-2.32	-16.55	4
PG1452+198	-14.94	-15.11	2
PG1519+640	-0.98	-3.85	2
PG1528+104	-1.98	-6.83	2
PG1558-007	-18.47	-18.47	3
PG1648+536	-7.10	-35.30	2
KUV16256+4034	-5.74	-13.96	2
EC20182-6534	-8.57	-10.04	2
EC20260-4757	-3.83	-3.83	5
EC20369-1804	-4.40	-4.83	2
KPD2040+3955	-2.75	-7.31	4
EC21556-5552	-8.43	-8.43	2
KPD2215+5037	-6.90	-20.88	2
EC22202-1834	-6.48	-9.21	2
EC22590-4819	-8.82	-8.82	2
PG2331+038	-4.75	-26.72	4

Table 4. T_{eff} , $\log g$ and $\log(\text{He}/\text{H})$. We list only values for the binary systems listed in Table 2 for which our data is sufficient to obtain a good constraint on these parameters.

Name	T_{eff} (K)	$\log g$	$\log(\text{He}/\text{H})$
PG0919+273	32900	5.90	-2.31
PG0934+186	35800	5.65	-3.00
PG1230+052	27100	5.47	-2.86
PG1244+113	36300	5.54	-3.00
PG1403+316	31200	5.75	-2.42
PG1452+198	29400	5.75	-2.00
PG1519+640	30600	5.72	-2.17
PG1528+104	27200	5.46	-2.52
PG1648+536	31400	5.62	-4.00
KUV16256+4034	23100	5.38	-2.99
KPD2040+3955	27900	5.54	-2.77
KPD2215+5037	29600	5.64	-2.24
PG2331+038	27200	5.58	-2.70

Table 5. For each binary, we list here the best-fit eccentricity (e) and the improvement in χ^2 compared to the circular orbit fit. In all cases, the improvement is not significant at the 95% level. We also give the upper bounds on e as determined from our MCMC calculation, at the 68, 95 and 99% confidence levels.

Name	e (best fit)	$\Delta\chi^2$	upper bound on e		
			68%	95%	99%
EC00404-4429	0.06	5.6	0.08	0.11	0.12
EC02200-2338	0.08	0.1	0.25	0.33	0.36
PG0919+273	0.01	0.6	0.03	0.05	0.07
PG0934+186	0.12	5.8	0.16	0.22	0.27
PG0958-073	0.06	0.6	0.12	0.19	0.24
PG1000+408	0.03	0.1	0.16	0.37	0.64
PG1230+052	0.02	0.6	0.05	0.07	0.09
EC12408-1427	0.06	1.3	0.08	0.14	0.17
PG1244+113	0.01	0.2	0.05	0.08	0.10
PG1253+284	0.13	7.5	0.16	0.23	0.27
EC13332-1424	0.03	1.2	0.05	0.07	0.09
PG1403+316	0.12	2.7	0.29	0.55	0.64
PG1439-013	0.13	3.8	0.19	0.32	0.41
PG1452+198	0.05	2.1	0.10	0.16	0.20
PG1519+640	0.13	11.7	0.15	0.20	0.23
PG1528+104	0.12	9.6	0.14	0.18	0.20
PG1558-007	0.06	5.5	0.08	0.11	0.13
PG1648+536	0.05	8.3	0.06	0.08	0.09
KUV16256+4034	0.05	4.9	0.07	0.10	0.12
EC20182-6534	0.06	1.5	0.10	0.16	0.19
EC20260-4757	0.05	1.0	0.11	0.19	0.34
EC20369-1804	0.03	0.2	0.09	0.16	0.21
KPD2040+3955	0.13	11.7	0.15	0.22	0.27
EC21556-5552	0.09	3.5	0.12	0.18	0.21
KPD2215+5037	0.04	3.8	0.05	0.08	0.10
EC22202-1834	0.15	4.5	0.19	0.27	0.33
EC22590-4819	0.03	0.6	0.06	0.10	0.12
PG2331+038	0.05	2.6	0.07	0.11	0.13

making significant detections of small eccentricities comparable to those reported by Edelmann et al. (2005). To investigate the limits of our data we used a Markov Chain Monte Carlo (MCMC) algorithm to perturb the elliptical orbit model parameters and compare to our radial velocity measurements. For each binary, we therefore determined the value of e for which our data is sufficient to give a significant detection. We list the results in Table 5. These are the upper bounds on e , at the 68, 95 and 99% confidence levels. With the exception of PG0919+273, we find the upper bound on e at the 95 and 99% levels is much greater than the range reported by Edelmann et al. (2005). We therefore cannot rule out small eccentricities comparable to those reported by Edelmann et al. (2005) in any of these binaries.

4.3 Unsolved systems, non-movers and the binary fraction

In Table 10 we list our radial velocity measurements for the 108 remaining sdBs which we have observed as a part of this project, but not previously published. In 88 of these systems, we detect no significant radial velocity variation. These systems are likely to be either single sdBs or binary systems in which the mass function is too low for us to detect radial velocity variations.

The remaining 20 sdBs do show significant radial ve-

locity variations, and we consider it likely that most or all of these are binaries. Our current data are not sufficient to distinguish the true orbital period in these systems from various competing aliases, and so these targets are prime candidates for future measurements. We mark these systems in Table 10 with an asterisk. Two systems of particular note are PG1610+519 and PG2317+046. The data we have collected to date suggest that the orbital periods of these systems may be relatively long at 50 – 70 days.

This list of twenty candidate binaries is not exhaustive. As we have previously discussed, some fraction of the ‘single’ sdBs may be long period systems. There are also a number of sdBs in Table 10 for which we only obtained a small number of measurements and in which there may be large radial velocity variations which we have missed. There are also some systems in which a small number of measurements suggest a radial velocity variation which is formally significant, but when we fit them we find the only possible aliases are very low in amplitude and imply a mass function which is unphysical for an sdB with a stellar companion. We do not mark such systems as binary candidates. However, some authors have discussed the possibility of close substellar companions to sdB stars. One such star in our sample is HD149382. Geier et al. (2009) inferred the presence of a close 8–23 M_J companion to this sdB using high-resolution radial velocity measurements, but the more recent data of Jacobs et al. (2011) found no such variation. Our data for this star do show radial velocity variations which are formally significant. However, we do not believe these data support the presence of a close companion, for two reasons. Firstly, HD149382 has a V -band magnitude of 8.9, making it by far the brightest star in our sample (the majority of our targets lie in the $12 > V > 14$ range). For such a bright star slit-filling errors are potentially larger than for faint stars because short exposures lead to larger deviations from the slit centre, and it is possible we have underestimated these in this case. Secondly, Jacobs et al. (2011) observed a red companion star with a 1” separation (~ 75 AU) from the sdB. Given we used a 1” slit, it is possible that our measurements were contaminated by this distant companion. In general, we believe our intermediate dispersion measurements are not sufficient to make convincing claims for any substellar companions to the sdBs in our sample.

As well as these 20 potential binaries and the 28 solved systems in this paper, we have previously published 23 binaries in Maxted et al. (2002) and Morales-Rueda et al. (2003). Additionally, there were 3 binaries which were originally on our target list but were since solved by other authors. Our best estimate for the binary fraction in the sdB population is therefore 46 per cent. This is a lower bound for the reasons discussed in the previous paragraph. In addition, some binaries were already known in the Palomar-Green catalogue of sdBs before our project began. Since we may have included these systems in our sample had they not already been solved, our sample is slightly biased *against* binary systems. Including these systems in our binary fraction increases the estimate to 49 per cent.

The initial study of the Palomar-Green sample of sdBs implied a binary fraction of 69 ± 9 per cent (Maxted et al. 2001). However, the sdB binary fraction determined from the SPY (ESO Supernovae type Ia Progenitor survey; Napiwotzki et al. 2001) sdB sample was found to contain

Table 6. The minimum companion masses M_{2min} and mass functions f_m for the 28 binary systems listed in Table 2, both in units of M_\odot . We also mark ‘WD’ the seven systems for which the companion star has been determined to be a white dwarf by ¹Maxted et al. (2004) or ²Shimanskii et al. (2008).

Object	M_{2min}	f_m	Companion
EC00404-4429	0.316	0.047	
EC02200-2338	0.389	0.074	
PG0919+273	0.480	0.115	
PG0934+186	0.430	0.092	
PG0958-073	0.142	0.007	
PG1000+408	0.250	0.028	WD ²
PG1230+052	0.132	0.006	WD ¹
EC12408-1427	0.212	0.019	
PG1244+113	0.439	0.096	
PG1253+284	0.123	0.005	
EC13332-1424	0.441	0.097	
PG1403+316	0.280	0.036	
PG1439-013	0.445	0.099	
PG1452+198	0.366	0.065	
PG1519+640	0.100	0.003	WD ¹
PG1528+104	0.127	0.005	WD ¹
PG1558-007	0.412	0.084	
PG1648+536	0.407	0.082	WD ¹
KUV16256+4034	0.101	0.003	WD ¹
EC20182-6534	0.183	0.013	
EC20260-4757	0.589	0.172	
EC20369-1804	0.362	0.064	
KPD2040+3955	0.505	0.128	WD ¹
EC21556-5552	0.234	0.024	
KPD2215+5037	0.333	0.053	
EC22202-1834	0.494	0.122	
EC22590-4819	0.470	0.110	
PG2331+038	0.452	0.102	

a binary fraction of 42 per cent (Napiwotzki et al. 2004). In comparing our binary fraction with the SPY result, we note that the SPY authors deliberately chose to exclude known composite spectrum objects from their survey. In Section 4.4 we report 32 composite objects in our target list. When we exclude these objects, our binary fraction increases to 53 – 56 per cent.

It was thought that the discrepancy between the (Maxted et al. 2001) and (Napiwotzki et al. 2004) binary fractions could be the result of the different populations surveyed in the two surveys, i.e. SPY looks at stars with white dwarf colours in the thick disk and halo whereas the Palomar-Green sample consists of targets with sdB colours in the thin disk. Our more extended study of the Palomar-Green sample (and the Edinburgh-Cape sample, which uses similar colour selection cuts) finds a binary fraction which is intermediate between the two earlier figures, and so we believe that the discrepancy is more likely due to low number statistics, rather than different populations being targeted. Finally, we note that the binary population synthesis of Han et al. (2003) predicted an observable binary frequency of 55 per cent for their best-fit simulation set (set 2) when selection effects are accounted for, which compares well with our finding.

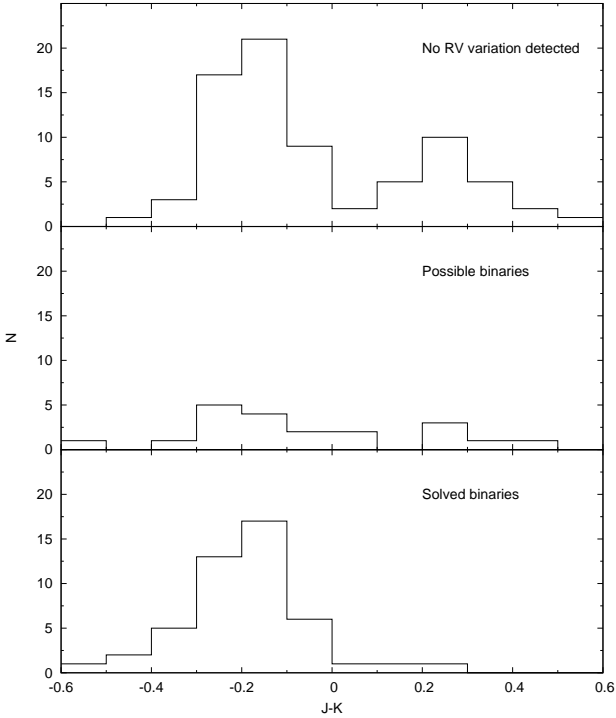


Figure 4. Histogram of the $J-K$ colours of the sdBs in our programme, obtained from 2MASS. We plot separately the 100 systems which show no significant radial velocity variation (top), the 25 systems which are candidate binaries but are currently unsolved (middle) and the solved binaries from this paper, Maxted et al. (2002) and Morales-Rueda et al. (2003) (bottom).

4.4 The nature of the companion stars

We combine the orbital periods and the radial velocity semi-amplitudes listed in Table 2 to calculate the mass function, f_m , of the system according to the well-known relation:

$$f_m = \frac{M_2^3 \sin^3 i}{(M_1 + M_2)^2} = \frac{PK_1^3}{2\pi G},$$

where the subscript ‘1’ refers to the sdB star and ‘2’ to its companion. If we take a canonical mass of $0.48M_\odot$ for the sdB star, we can also calculate the minimum mass of its companion, $M_{2\min}$. The values for f_m and $M_{2\min}$ obtained in each case are given in Table 6. Additionally, we indicate seven systems for which the companion has been determined to be a white dwarf through the photometric studies of Maxted et al. (2004) or Shimanskii et al. (2008), which showed an absence of reflection effects in these systems, implying a degenerate companion.

Some fraction of the sdB population are composite systems, in which flux excesses at long wavelengths or spectral features indicate the presence of a cool, G-K-type companion. The remaining ‘single’ sdBs may truly be single stars, or they may have unseen white dwarf or fainter, dM-type companions. Using Two Micron All Sky Survey (2MASS)¹ observations, Stark & Wade (2003) showed the composite

and ‘single’ sdB populations can be distinguished by their $J-K_s$ colour, with the ‘single’ stars having $J-K_s < +0.05$ and the composites having $J-K_s > +0.05$. In figure 7 of Stark & Wade (2003) a histogram of the $J-K_s$ colours of all of the sdBs in the 2MASS Second Incremental Data Release showed a clear bimodal distribution. In Figure 4 we reproduce this histogram for the sdBs in our programme. We plot separately the sdBs which show no radial velocity variations, the sdBs which are strong binary candidates but without an orbital period determination, and the solved binaries, comprising the 28 systems from this paper and those previously published in Maxted et al. (2002) and Morales-Rueda et al. (2003). We exclude from this histogram the Kitt Peak-Downes (KPD; Downes 1986) survey objects, since they are close to the galactic plane and thus potentially significantly reddened.

If we examine first the histogram for the sdBs which shown no radial velocity variation, we see the same bimodal distribution around a $J-K_s$ value of $+0.05$ as was found in Stark & Wade (2003). By comparison, the histogram of the solved binaries shows only two systems with $J-K_s > +0.05$: PG1253+284 and PG1558-007. PG1558-007 was identified as a composite system by Allard et al. (1994), but Heber et al. (2002) disputed this identification, attributing the $J-K_s$ colour to interstellar reddening. PG1253+284 was identified as a composite system by Ulla & Thejll (1998), but for this system Heber et al. (2002) determined PG1253+284 (referred to as TON 139 in that paper) to be a triple system via *HST* imaging, and concluded that the $J-K_s$ colour in this system is due to the third, distant component, and not the companion in the close binary. The third histogram (the potential but unsolved binaries) indicates the presence of a further five composite systems. Aside from the possibility that these are close binaries with a G-K companion, there are three explanations for these measurements. Firstly, some of these composite sdBs may not actually be close binaries: further observations may show the radial velocity variations detected to date are not significant. Secondly, some of the $J-K_s$ measurements may be due to a third component, interstellar reddening or a nearby unresolved field star. Thirdly, some of these unsolved binaries may actually be long period systems, as we noted in Section 4.3.

To investigate this further, we generated mean spectra for all of the objects in our target list, and classified them with the aid of synthetic spectra from the grid described in Section 4.1. 25 objects show contamination in their spectra indicative of a cool companion, which would indicate these are composite systems. We would classify these sdBs as ‘double-lined spectroscopic binaries’, to distinguish them from the single-lined spectroscopic binaries, the nature of which we identify via radial velocity variations. There is strong overlap between the double-lined spectroscopic binaries and the composite systems we identified through 2MASS, with all but five of the 2MASS systems showing a contaminating component in their spectra. We list our candidate composite binaries in Table 7. We exclude PG2059+013 from this table: while the $J-K_s$ colour of this sdB is consistent with it being a composite system, but the Schlegel et al. (1998) dust maps show it to be significantly reddened. This table contains five systems in which

¹ At <http://www.ipac.caltech.edu/2mass>.

Table 7. sdBs in our sample which show evidence for being composite systems. All of the sdBs we list have 2MASS colours which indicate a cool companion. The majority of these systems are ‘double-lined’ binaries, in which the inspection of our own spectra show evidence for a contaminating component. The four systems we list at the end show no such evidence. We also embolden the five objects which show some evidence for binarity through radial velocity variations.

PG0039+049	EC20117-4014
PB8783	EC20228-3628
EC03143-5945	EC20387-1716
EC03238-0710	EC21079-3548
EC04170-3433	PG2110+127
EC04515-3754	PG2118+126
EC05053-2806	EC21373-3727
PG0749+658	PG2148+095
EC09436-0929	PG2226+094
PG1040+234	
EC12473-3046	2MASS only
PG1338+611	EC03470-5039
PG1551+256	PG1526+132
PG1610+519	EC22133-6446
PG1618+563	PG2317+046
PG1701+359	

we believe we detect significant radial velocity variations, and hence are potentially close binaries.

In summary then, almost all of the systems which we identify as close binaries do not show the presence of a dwarf G-K companion. The companions in these systems are therefore most likely white dwarfs or M dwarfs. The composite systems are almost entirely found in the group of sdBs in which we detected no radial velocity variations. A G-K companion therefore seems to be indicative of a longer period system: a wide binary in which the sdB has evolved independently of the companion. There are some potential exceptions to this rule: these sdBs are prime candidates for further observation in order to determine if they are indeed binaries, as the data collected to date would suggest, and furthermore if they are close binaries. As we remarked in Section 4.3, two of these candidates (PG1610+519 and PG2317+046) show evidence for binarity, but all of the current aliases suggest a long orbital period, which would be consistent with our composite identification.

4.5 Misclassifications in the literature

Our main source for the construction of our target list was Kilkenny et al. (1988), with the Edinburgh Cape objects coming from Kilkenny et al. (1997) and private communications. Over the course of our study we discovered a number of sources which have been misidentified as sdB stars in these catalogues, which we list in Table 8. At the time of writing they are all still listed as sdBs in the SIMBAD astronomical database, although the misidentification has previously been reported for six of these eleven objects. For the other five we give our new classifications, obtained using the same spectral fitting techniques described in Section 4.1.

Table 8. Ten objects in our survey which were misidentified as sdB stars in Kilkenny et al. (1988) or Kilkenny et al. (1997). Six of these objects have previously been reclassified by ¹Gianninas et al. (2010), ²Saffer et al. (1997) or ³Ramspeck et al. (2001).

Object	Our classification
KPD 0311+4801	DA, $T_{\text{eff}} = 97080\text{K}$, $\log g = 6.96$ ¹
KUV 04110+1434	MS B-star, $T_{\text{eff}} = 13000\text{K}$
UVO0653-23	B-star
KPD 0721-0026	B-star, $T_{\text{eff}} = 11868\text{K}$, $\log g = 3.68$ ²
HD 80836	MS B-star
EC10282-1605	MS B-star, $T_{\text{eff}} \sim 16000\text{K}$
EC13506-3137	sdO star of unusually low gravity
PG1533+467	MS B-star, $T_{\text{eff}} = 18100\text{K}$, $\log g = 4.00$ ³
KPD 2022+2033	B-star, $T_{\text{eff}} = 16752\text{K}$, $\log g = 4.46$ ²
PG2111+023	MS B-star, $T_{\text{eff}} = 18305\text{K}$, $\log g = 4.5$ ²
PG2301+259	MS B-star, $T_{\text{eff}} = 17901\text{K}$, $\log g = 4.11$ ²

5 CONCLUSIONS

In this paper we present a large number of radial velocity measurements of bright sdB stars. The aim of this project was to detect binary systems through variations in these radial velocity measurements, and hence determine the orbital parameters of those systems. This is a continuation of the work begun in Maxted et al. (2002) and Morales-Rueda et al. (2003). We presented a total of 28 new binary systems with their parameters, in all cases determining the orbital period to much better than 5 per cent. We determined effective temperatures and surface gravities for 13 of the sdBs in these systems. The parameters are consistent with the sdBs being extreme horizontal branch stars (EHB) with two exceptions, PG0934+186 and PG1244+113, which we classify as post-EHB stars.

As well as the 28 solved systems we presented measurements for 108 other sdBs. 20 of these show strong signs of binarity, but our data is insufficient as yet to constrain the system parameters. The remaining 100 stars show no significant radial velocity variations and are likely to be either single sdBs or binary systems in which the orbital period is long enough to push the radial velocity variations below our detection threshold. Our best estimate for the binary fraction is 46 – 56 per cent. Finally, we note that none of the binaries we report in this paper show the near-infrared colours which indicate the presence of a G-K-type companion star. The companion stars in our solved systems are therefore likely either white dwarfs or M dwarfs. There is some evidence for a cool companion in the spectra of 32 of the remaining sdBs, including 5 which show radial velocity variations. These are strong candidates for future study.

ACKNOWLEDGEMENTS

CMC and TRM are supported under grant ST/F002599/1 from the Science and Technology Facilities Council (STFC). The results presented in this paper are based on observations made with the Isaac Newton Telescope operated on the island of La Palma by the Isaac Newton Group in the Spanish Observatorio del Roque de los Muchachos of the Instituto de Astrofísica de Canarias and observations made with the

1.9 m telescope operated by the South African Astronomical Observatory. This research has made use of NASA's Astrophysics Data System Bibliographic Services and the SIMBAD database, operated at CDS, Strasbourg, France. This publication makes use of data products from the Two Micron All Sky Survey, which is a joint project of the University of Massachusetts and the Infrared Processing and Analysis Center/California Institute of Technology, funded by the National Aeronautics and Space Administration and the National Science Foundation. We thank the referee for helpful comments.

REFERENCES

- Allard F., Wesemael F., Fontaine G., Bergeron P., Lamontagne R., 1994, *AJ*, 107, 1565
- Cumming A., Marcy G. W., Butler R. P., 1999, *ApJ*, 526, 890
- D'Cruz N. L., Dorman B., Rood R. T., O'Connell R. W., 1996, *ApJ*, 466, 359
- Downes R. A., 1986, *ApJS*, 61, 569
- Edelmann H., Heber U., Altmann M., Karl C., Lisker T., 2005, *A&A*, 442, 1023
- Geier S., Edelmann H., Heber U., Morales-Rueda L., 2009, *ApJL*, 702, L96
- Gianninas A., Bergeron P., Dupuis J., Ruiz M. T., 2010, *ApJ*, 720, 581
- Green E. M., Liebert J., Saffer R. A., 2001, in J. L. Provençal, H. L. Shipman, J. MacDonald, & S. Goodchild ed., 12th European Workshop on White Dwarfs Vol. 226 of *Astronomical Society of the Pacific Conference Series*, On The Origin Of Subdwarf B Stars and Related Metal-Rich Binaries. p. 192
- Han Z., Podsiadlowski P., Maxted P. F. L., Marsh T. R., 2003, *MNRAS*, 341, 669
- Han Z., Podsiadlowski P., Maxted P. F. L., Marsh T. R., Ivanova N., 2002, *MNRAS*, 336, 449
- Heber U., 2009, *ARAA*, 47, 211
- Heber U., Hunger K., Jonas G., Kudritzki R. P., 1984, *A&A*, 130, 119
- Heber U., Moehler S., Napiwotzki R., Thejll P., Green E. M., 2002, *A&A*, 383, 938
- Heber U., Reid I. N., Werner K., 2000, *A&A*, 363, 198
- Iben Jr. I., Livio M., 1993, *PASP*, 105, 1373
- Jacobs V. A., Østensen R. H., Van Winckel H., Bloemen S., Pápics P. I., Raskin G., Deboscher J., Uttenthaler S., Van Aarle E., Waelkens C., Bauwens E., Verhoelst T., Gielen C., Lehmann H., Oreiro R., 2011, *ArXiv e-prints*
- Kilkenny D., Heber U., Drilling J. S., 1988, *South African Astronomical Observatory Circular*, 12, 1
- Kilkenny D., O'Donoghue D., Koen C., Stobie R. S., Chen A., 1997, *MNRAS*, 287, 867
- Lomb N. R., 1976, *Ap&SS*, 39, 447
- Marsh T. R., 1989, *PASP*, 101, 1032
- Marsh T. R., Dhillon V. S., Duck S. R., 1995, *MNRAS*, 275, 828
- Maxted P. f. L., Heber U., Marsh T. R., North R. C., 2001, *MNRAS*, 326, 1391
- Maxted P. F. L., Marsh T. R., Heber U., Morales-Rueda L., North R. C., Lawson W. A., 2002, *MNRAS*, 333, 231
- Maxted P. F. L., Marsh T. R., Moran C. K. J., 2000, *MNRAS*, 319, 305
- Maxted P. F. L., Morales-Rueda L., Marsh T. R., 2004, *Ap&SS*, 291, 307
- Morales-Rueda L., Marsh T. R., North R. C., Maxted P. F. L., 2003, in D. de Martino, R. Silvotti, J.-E. Solheim, & R. Kalytis ed., *NATO ASIB Proc. 105: White Dwarfs New subdwarf B star periods*. p. 57
- Morales-Rueda L., Maxted P. F. L., Marsh T. R., Kilkenny D., O'Donoghue D., 2005, in D. Koester & S. Moehler ed., 14th European Workshop on White Dwarfs Vol. 334 of *Astronomical Society of the Pacific Conference Series*, Subdwarf B Binaries from the Edinburgh-Cape Survey. p. 333
- Morales-Rueda L., Maxted P. F. L., Marsh T. R., Kilkenny D., O'Donoghue D., 2006, *Baltic Astronomy*, 15, 187
- Morales-Rueda L., Maxted P. F. L., Marsh T. R., North R. C., Heber U., 2003, *MNRAS*, 338, 752
- Napiwotzki R., Christlieb N., Drechsel H., Hagen H., Heber U., Homeier D., Karl C., Koester D., Leibundgut B., Marsh T. R., Moehler S., Nelemans G., Pauli E., Reimers D., Renzini A., Yungelson L., 2001, *Astronomische Nachrichten*, 322, 411
- Napiwotzki R., Karl C. A., Lisker T., Heber U., Christlieb N., Reimers D., Nelemans G., Homeier D., 2004, *Ap&SS*, 291, 321
- O'Toole S. J., Heber U., 2006, *A&A*, 452, 579
- Press W. H., 2002, *Numerical recipes in C++ : the art of scientific computing*. Cambridge University Press
- Pretorius M. L., Knigge C., Kolb U., 2007, *MNRAS*, 374, 1495
- Ramspeck M., Heber U., Moehler S., 2001, *A&A*, 378, 907
- Saffer R. A., Bergeron P., Koester D., Liebert J., 1994, *ApJ*, 432, 351
- Saffer R. A., Keenan F. P., Hambly N. C., Dufton P. L., Liebert J., 1997, *ApJ*, 491, 172
- Scargle J. D., 1982, *ApJ*, 263, 835
- Schlegel D. J., Finkbeiner D. P., Davis M., 1998, *ApJ*, 500, 525
- Shimanskii V. V., Bikmaev I. F., Borisov N. V., Vlasyuk V. V., Galeev A. I., Sakhbullin N. A., Spiridonova O. I., 2008, *Astronomy Reports*, 52, 729
- Stark M. A., Wade R. A., 2003, *AJ*, 126, 1455
- Tutukov A. V., Yungelson L. R., 1981, *Nauchnye Informatsii*, 49, 3
- Ulla A., Thejll P., 1998, *AAPS*, 132, 1
- Webbink R. F., 1984, *ApJ*, 277, 355
- Yungelson L. R., Tutukov A. V., 2005, *Astronomy Reports*, 49, 871

Table 9. Radial velocity measurements for the 28 sdB binaries which we present in this paper.

HMJD	RV (km s ⁻¹)	HMJD	RV (km s ⁻¹)	HMJD	RV (km s ⁻¹)	HMJD	RV (km s ⁻¹)
<u>EC00404-4429</u>		<u>PG0919+273</u>		<u>PG1000+408</u>		<u>PG1244+113</u>	
52892.9858	-124.51 ± 5.13	54902.9529	-74.14 ± 1.26	54191.9382	28.74 ± 2.11	51654.1003	-21.09 ± 5.70
52893.0000	-78.05 ± 5.11	54902.9704	-74.38 ± 1.26	54191.9522	33.23 ± 2.00	51977.1722	-32.37 ± 9.29
52893.1529	96.73 ± 4.86	<u>PG0934+186</u>		<u>PG1230+052</u>		51977.1827	-48.06 ± 9.30
52893.1671	161.87 ± 5.97	52360.9826	67.29 ± 3.19	52387.9376	-85.66 ± 11.24	51982.1343	-20.65 ± 6.05
52893.9884	-28.82 ± 4.12	52360.9966	70.62 ± 3.21	52387.9534	-78.37 ± 8.46	51982.1448	-17.57 ± 5.95
52894.0041	-113.13 ± 4.23	52361.0510	66.46 ± 2.65	52390.9528	-7.95 ± 2.09	51982.2290	-11.29 ± 7.18
52894.0197	-106.96 ± 4.23	52361.0650	67.23 ± 2.58	52390.9635	-8.77 ± 2.87	51982.2394	-10.75 ± 7.49
52896.9267	58.39 ± 5.80	52361.9272	3.88 ± 3.17	52390.9973	-12.45 ± 3.94	52030.9039	54.66 ± 10.34
52896.9409	-32.49 ± 5.36	52361.9343	3.64 ± 2.95	52391.0045	-11.92 ± 3.54	52030.9144	34.65 ± 10.91
<u>EC02200-2338</u>		52361.9683	4.40 ± 2.86	52391.8989	-20.38 ± 1.83	52032.0570	60.34 ± 4.50
52893.0509	-28.99 ± 2.08	52361.9754	5.34 ± 2.82	52391.9096	-30.06 ± 1.94	52032.0726	53.38 ± 6.78
52893.0617	-24.97 ± 2.10	52362.0590	-15.04 ± 3.03	52391.9831	-52.42 ± 2.16	52036.0392	-8.67 ± 13.21
52894.0688	107.97 ± 1.75	52362.0661	-11.18 ± 3.39	52391.9903	-56.15 ± 2.12	52036.0545	3.31 ± 7.99
52894.0795	110.91 ± 1.81	52387.8990	-27.67 ± 9.85	52392.1596	-88.17 ± 9.54	52036.0693	8.56 ± 5.67
52896.9574	-72.84 ± 2.39	52387.9096	-24.38 ± 8.36	52393.1168	-72.13 ± 3.98	52037.0903	58.40 ± 8.37
52896.9680	-73.29 ± 2.41	52389.9387	31.38 ± 8.96	52393.1240	-72.62 ± 3.94	52037.1007	68.93 ± 9.54
52897.1604	41.92 ± 2.34	52389.9494	31.72 ± 9.73	52394.0944	-25.06 ± 2.23	52037.9680	58.30 ± 15.66
52897.1710	47.89 ± 3.26	52391.9454	-20.38 ± 2.26	52394.1016	-26.25 ± 2.26	52038.0319	38.46 ± 8.41
52897.9449	30.21 ± 2.64	52391.9561	-20.29 ± 2.04	52394.9025	-35.08 ± 2.56	52038.0681	66.28 ± 9.72
52897.9570	33.80 ± 2.41	52392.8678	53.23 ± 2.88	52394.9097	-36.52 ± 2.49	52390.9009	-44.48 ± 3.58
<u>PG0919+273</u>		52392.8750	51.52 ± 2.93	54186.1483	-67.97 ± 5.52	52390.9150	-44.56 ± 3.26
51652.8518	-77.20 ± 4.07	<u>PG0958-073</u>		54186.1589	-74.42 ± 4.93	52391.0531	-38.86 ± 6.66
51652.8562	-83.25 ± 3.84	52362.8649	97.72 ± 4.05	54188.9017	-45.82 ± 3.72	52391.0672	-59.23 ± 7.39
51653.9461	-57.47 ± 3.21	52362.8766	107.06 ± 4.10	54188.9122	-63.98 ± 2.45	52392.9466	19.61 ± 5.07
51653.9505	-58.29 ± 3.15	52363.8644	107.47 ± 4.95	54190.0697	-9.41 ± 2.04	52392.9538	15.33 ± 4.91
52361.8796	-51.08 ± 3.74	52363.8762	106.10 ± 4.62	54190.0803	-8.91 ± 1.90	54185.1282	-19.35 ± 4.23
52361.8832	-59.99 ± 3.22	54189.9787	102.64 ± 2.01	54191.0239	-37.35 ± 2.17	54185.1422	-22.98 ± 3.98
52361.9143	-54.96 ± 3.57	54189.9928	97.55 ± 2.05	54191.0344	-40.40 ± 2.39	54187.9900	29.69 ± 7.38
52361.9179	-51.01 ± 3.56	54544.9753	102.47 ± 2.62	<u>EC12408-1427</u>		54188.0040	33.74 ± 2.91
52364.8420	-90.86 ± 5.55	54544.9894	103.73 ± 2.34	52359.9674	8.30 ± 5.73	54191.0610	-44.49 ± 4.35
52364.8491	-91.81 ± 4.45	54546.9353	68.73 ± 3.49	52359.9791	0.21 ± 5.97	54191.0802	-36.60 ± 2.28
52387.8743	-39.18 ± 4.36	54546.9529	58.76 ± 2.68	52363.9527	-90.29 ± 4.04	54196.0172	6.74 ± 2.57
52387.8850	-43.35 ± 3.89	54903.9622	72.19 ± 1.83	52363.9633	-98.45 ± 4.34	54196.0381	9.68 ± 2.50
52389.8909	-30.85 ± 2.62	54903.9762	71.23 ± 1.74	52364.0110	-113.52 ± 5.07	54197.0684	-43.90 ± 3.41
52389.8981	-26.64 ± 2.70	54905.9308	74.35 ± 1.60	52364.0217	-115.04 ± 5.64	54197.0859	-48.21 ± 2.77
52391.9656	-34.87 ± 2.84	54905.9518	82.43 ± 1.66	52364.9004	-110.89 ± 2.71	54544.1241	-2.47 ± 2.89
54184.8900	-51.89 ± 2.11	54906.0913	83.40 ± 2.13	52364.9099	-107.96 ± 2.79	54544.1381	14.10 ± 2.83
54184.9006	-53.22 ± 2.17	54906.1106	79.36 ± 2.55	52364.9700	-104.87 ± 3.02	54901.0952	26.49 ± 10.20
54185.8630	-71.15 ± 2.81	54906.9068	70.36 ± 0.81	52364.9783	-109.31 ± 3.17	54901.1162	6.13 ± 10.76
54185.9145	-69.80 ± 2.37	54906.9278	71.31 ± 2.31	52365.1026	-83.42 ± 6.50	54901.1607	30.62 ± 9.24
54186.9793	-91.95 ± 2.41	54906.9976	71.11 ± 1.90	52365.1109	-79.30 ± 5.76	54904.0400	-15.81 ± 3.78
54186.9898	-84.68 ± 2.54	54907.0185	74.90 ± 2.57	52719.0414	-11.55 ± 3.49	54904.0610	-13.37 ± 7.22
54188.9296	-106.43 ± 1.49	54907.0419	71.59 ± 2.06	52719.0520	-9.66 ± 3.53	54904.0843	-8.45 ± 6.61
54188.9401	-109.01 ± 1.50	<u>PG1000+408</u>		52720.0622	7.57 ± 5.20	54906.1353	-4.33 ± 3.77
54189.8946	-113.90 ± 1.71	51648.8644	80.31 ± 16.63	52720.0728	8.58 ± 5.38	54906.1494	-3.53 ± 3.78
54189.9051	-108.21 ± 1.75	51648.8687	79.03 ± 13.64	53095.8583	-117.18 ± 6.85	54951.9511	-21.41 ± 1.94
54192.9248	-84.69 ± 1.44	51650.8991	101.74 ± 6.12	53095.8797	-109.81 ± 10.61	54951.9651	-21.32 ± 1.90
54192.9353	-80.55 ± 1.38	51650.9054	101.82 ± 5.91	53101.0041	40.10 ± 51.44	54951.9778	-15.29 ± 2.58
54196.8596	-30.57 ± 1.71	51650.9197	92.60 ± 6.46	53101.0148	-47.01 ± 55.80	<u>PG1253+284</u>	
54196.8702	-29.34 ± 1.69	51650.9260	91.82 ± 6.27	53101.9736	-21.44 ± 14.52	52393.8556	-7.91 ± 2.85
54900.8833	-42.30 ± 1.51	51655.8593	78.81 ± 7.08	53101.9843	-49.64 ± 15.96	52393.8628	-4.66 ± 2.21
54900.9043	-35.82 ± 2.30	51655.8661	112.09 ± 7.10	53102.9589	-70.09 ± 2.67	52394.0000	-1.98 ± 1.21
54900.9271	-45.03 ± 1.81	51656.8492	70.89 ± 6.34	53102.9800	-71.58 ± 4.17	52394.0106	-5.39 ± 1.27
54900.9481	-46.61 ± 2.35	51656.8575	84.64 ± 5.46	53546.7334	28.67 ± 32.01	52394.9430	22.07 ± 1.16
54901.0388	-41.93 ± 3.19	54185.9322	114.52 ± 3.13	53546.7490	-15.70 ± 11.63	52394.9571	23.00 ± 1.15
54901.0597	-36.78 ± 3.16	54185.9462	117.23 ± 2.62	53546.7664	-19.69 ± 26.73	54186.1194	-7.66 ± 3.73
54901.8701	-57.47 ± 2.58	54188.0181	117.70 ± 1.97	53548.7051	-50.43 ± 5.21	54186.1789	-6.99 ± 7.96
54901.8911	-56.96 ± 1.74	54188.0321	119.15 ± 2.15	53548.7196	-52.11 ± 5.07	54188.1001	16.52 ± 1.12
54901.9788	-55.82 ± 2.36	54188.8607	56.51 ± 3.41	<u>PG1244+113</u>		54188.1141	17.55 ± 1.10
54901.9998	-59.26 ± 2.15	54188.8747	59.13 ± 2.54	51646.0409	65.12 ± 5.56	54189.0028	-3.40 ± 0.95
54902.0231	-51.54 ± 2.65	54189.8591	36.54 ± 2.22	51646.0505	68.70 ± 5.79	54189.0168	-3.73 ± 0.91
54902.0441	-50.07 ± 2.65	54189.8732	44.35 ± 2.24	51654.0907	-13.70 ± 6.66	54190.1043	44.29 ± 1.09

Table 9. Radial velocity measurements for the 28 sdB binaries which we present in this paper.

HMJD	RV (km s ⁻¹)	HMJD	RV (km s ⁻¹)	HMJD	RV (km s ⁻¹)	HMJD	RV (km s ⁻¹)
<u>PG1253+284</u>		<u>PG1439-013</u>		<u>PG1519+640</u>		<u>PG1558-007</u>	
54190.1183	43.52 ± 1.08	52360.0982	-109.88 ± 15.03	52390.9823	38.86 ± 2.47	53103.0441	-99.63 ± 2.87
54191.1132	15.61 ± 0.85	52363.0472	-5.19 ± 9.27	52391.0106	35.96 ± 4.38	53103.0651	-101.28 ± 2.96
54191.1255	17.70 ± 1.00	52363.0578	-14.69 ± 10.56	52391.0143	35.17 ± 5.33	53543.9387	-60.22 ± 8.61
54193.9361	18.93 ± 0.91	52719.9969	-28.05 ± 12.92	52391.0180	30.89 ± 5.72	53543.9531	-51.02 ± 9.63
54193.9501	19.01 ± 0.91	52720.0110	1.88 ± 13.70	52391.0217	34.95 ± 4.61	53544.8236	-88.18 ± 6.64
54195.0801	-2.82 ± 1.17	52721.1381	-40.15 ± 15.78	52391.1023	11.34 ± 2.82	53544.8377	-91.40 ± 6.35
54195.0941	-2.57 ± 1.21	52721.1555	-29.99 ± 17.16	52391.1129	12.92 ± 2.43	54185.2330	-59.72 ± 1.83
54544.2634	8.98 ± 1.09	54187.2025	-30.06 ± 4.24	52391.1236	-2.39 ± 2.30	54185.2561	-56.59 ± 2.57
54544.2774	6.86 ± 1.37	54187.2130	-36.47 ± 6.69	52391.2178	-35.83 ± 1.72	54188.2227	-112.46 ± 1.86
54553.0913	17.50 ± 3.32	54188.1291	-77.06 ± 3.91	52391.2285	-36.85 ± 1.77	54188.2368	-123.80 ± 1.85
54553.1054	5.45 ± 4.06	54188.1397	-77.72 ± 3.85	52392.0016	24.74 ± 1.95	<u>PG1648+536</u>	
54553.1217	4.33 ± 4.66	54189.1089	-99.58 ± 3.88	52392.0088	31.94 ± 1.69	52394.1708	-79.50 ± 2.16
54553.1358	13.39 ± 6.35	54189.1195	-95.59 ± 4.03	52392.2246	-16.38 ± 3.67	52394.1850	-64.36 ± 2.15
54904.1128	1.30 ± 2.53	54190.1324	-90.95 ± 3.31	52392.2283	-15.59 ± 3.78	52394.9886	21.58 ± 3.64
54904.1268	0.88 ± 1.42	54190.1430	-96.19 ± 3.34	<u>PG1528+104</u>		52394.9993	15.69 ± 3.30
54904.1555	3.89 ± 1.00	54194.0632	-14.17 ± 2.96	52394.0261	-21.63 ± 2.14	52395.0745	-49.68 ± 3.59
54904.1695	4.61 ± 0.99	54194.0738	-16.21 ± 3.12	52394.0368	-32.06 ± 2.16	52395.0852	-67.88 ± 3.36
54951.9998	-12.82 ± 0.54	54194.1785	-25.47 ± 3.35	52394.1208	-96.93 ± 2.58	52395.1288	-107.80 ± 3.00
54952.0127	-6.84 ± 0.64	54194.1890	-25.31 ± 3.44	52394.1280	-99.33 ± 2.57	52395.1395	-124.28 ± 3.48
<u>EC13332-1424</u>		54194.9956	-45.77 ± 3.93	52394.2024	-73.71 ± 2.50	52395.1722	-145.89 ± 4.09
52363.0216	-155.91 ± 6.04	54195.0062	-44.86 ± 3.68	52394.2096	-65.22 ± 2.49	52395.1829	-143.67 ± 4.16
52363.0323	-152.81 ± 5.70	54195.1788	-70.63 ± 3.09	52394.2355	-27.17 ± 4.89	52395.1948	-161.91 ± 4.21
52365.0258	18.54 ± 3.49	54195.1975	-63.45 ± 3.19	52394.2385	-21.96 ± 5.20	54189.1981	45.25 ± 1.70
52365.0399	22.39 ± 3.47	54196.0543	-99.24 ± 2.85	52394.2444	-20.56 ± 5.81	54189.2156	38.45 ± 2.32
52365.0767	44.76 ± 5.03	54196.0683	-97.67 ± 2.94	52394.2474	-23.83 ± 6.70	54194.0212	22.88 ± 1.96
52365.0884	52.69 ± 5.82	54544.1851	-26.81 ± 3.08	52394.9724	2.72 ± 3.08	54194.0422	29.17 ± 1.83
52719.0138	-145.30 ± 5.81	54544.1991	-24.84 ± 3.21	52394.9796	3.16 ± 3.19	54905.2272	23.34 ± 2.35
52719.0244	-138.72 ± 5.43	54545.2409	-65.42 ± 3.76	52395.0579	-56.44 ± 3.59	54905.2481	10.15 ± 1.88
52720.1602	-21.03 ± 14.31	54545.2550	-74.41 ± 2.90	52395.0651	-66.74 ± 3.33	54906.2541	-51.00 ± 3.81
52720.1709	-32.34 ± 21.87	54545.2746	-77.45 ± 5.14	<u>PG1558-007</u>		54906.2699	-37.40 ± 4.74
53095.9061	-100.89 ± 11.02	54901.1879	3.93 ± 10.56	52363.0998	-53.35 ± 4.77	54907.1534	-64.02 ± 2.84
53095.9272	-117.66 ± 22.13	54901.2089	-25.17 ± 10.10	52363.1139	-42.38 ± 5.08	54907.1709	-85.85 ± 2.86
53099.9697	-166.82 ± 9.09	54902.1478	-48.62 ± 4.57	52365.1246	-91.64 ± 4.52	<u>KUV16256+4034</u>	
53099.9839	-152.39 ± 6.60	54902.1722	-44.25 ± 4.30	52365.1364	-95.26 ± 4.80	52390.0852	-100.88 ± 1.81
53102.0324	45.80 ± 7.99	54902.1976	-52.51 ± 4.38	52365.1493	-116.79 ± 5.67	52390.1063	-92.64 ± 1.32
53102.0535	28.58 ± 9.74	54902.2186	-48.68 ± 3.98	52720.1184	-94.85 ± 9.57	52391.0316	-104.73 ± 3.20
53103.0057	-30.37 ± 5.38	<u>PG1452+198</u>		52720.1325	-100.38 ± 9.97	52391.0370	-117.84 ± 3.41
53103.0268	-51.83 ± 4.61	52129.8666	-85.36 ± 1.60	52740.0952	-106.39 ± 2.62	52391.1596	-55.83 ± 1.85
53544.7500	-45.95 ± 14.60	52129.8736	-84.52 ± 1.61	52740.1059	-104.39 ± 2.61	52391.1703	-50.52 ± 1.72
53544.7642	-36.59 ± 16.27	52130.8653	-77.72 ± 2.36	52743.1068	-40.45 ± 6.52	52392.0236	-91.67 ± 1.22
53545.8428	42.44 ± 10.02	52130.8730	-75.80 ± 2.39	52744.0989	-28.24 ± 4.19	52392.0342	-87.38 ± 1.31
53545.8569	27.77 ± 10.80	52363.2145	-70.30 ± 6.48	52744.1084	-37.38 ± 4.60	52392.2046	-67.39 ± 1.41
<u>PG1403+316</u>		52363.2183	-81.25 ± 6.24	52744.1535	-34.79 ± 3.31	52392.2153	-74.06 ± 1.38
52393.8996	36.24 ± 3.71	52387.9709	88.75 ± 9.54	52744.1653	-29.95 ± 3.24	52392.9629	-96.40 ± 2.12
52393.9068	34.68 ± 3.39	52387.9816	75.69 ± 5.36	52745.0541	-25.33 ± 3.01	52392.9701	-89.53 ± 2.02
52395.0143	5.30 ± 2.78	52388.0467	53.95 ± 3.41	52745.0647	-28.71 ± 2.79	52393.0702	-49.53 ± 1.71
52395.0215	-1.45 ± 2.62	52388.0608	41.67 ± 2.98	52745.1642	-33.13 ± 2.27	52393.0774	-50.74 ± 1.70
52395.1003	18.09 ± 3.20	52389.9907	47.50 ± 3.96	52745.1760	-35.09 ± 2.30	52394.2178	-110.64 ± 1.30
52395.1075	22.83 ± 3.45	52389.9979	40.25 ± 4.29	52745.2281	-30.03 ± 2.70	52394.2250	-117.45 ± 1.35
52395.1547	26.11 ± 3.74	52390.0596	15.29 ± 3.46	52747.0890	-65.50 ± 3.13	52395.2201	-127.88 ± 1.96
52395.1619	30.42 ± 3.65	52390.0668	5.10 ± 4.61	52747.1013	-64.13 ± 2.55	52395.2273	-127.28 ± 2.10
54187.1596	-39.00 ± 1.94	52390.9380	55.73 ± 3.21	52747.1176	-67.88 ± 3.15	<u>EC20182-6534</u>	
54187.1806	-36.08 ± 2.06	52390.9417	53.66 ± 3.16	52747.1282	-65.71 ± 3.39	52896.8455	35.31 ± 5.78
54193.9656	-58.24 ± 1.46	52392.0960	-34.22 ± 3.75	52746.2195	-39.57 ± 2.36	52896.8561	32.46 ± 5.13
54193.9866	-55.08 ± 1.43	52392.0998	-52.67 ± 2.55	52892.7187	-84.44 ± 3.86	52897.8218	40.52 ± 6.68
54194.2050	-20.80 ± 1.41	52395.2096	-92.54 ± 3.75	52892.7333	-83.42 ± 3.59	52897.8324	44.59 ± 6.77
54194.2260	-13.98 ± 1.78	52395.2133	-94.66 ± 3.70	52893.7168	-113.83 ± 4.22	53301.7904	-14.56 ± 18.41
54194.9545	44.41 ± 1.96	<u>PG1519+640</u>		52893.7310	-104.84 ± 3.65	53301.8041	-40.34 ± 10.65
54194.9685	36.62 ± 1.89	52390.1887	-34.63 ± 1.92	52894.7206	-122.43 ± 9.74	53302.7609	76.03 ± 5.85
<u>PG1439-013</u>		52390.2261	-28.40 ± 2.17	52895.7187	-108.77 ± 4.09	53302.7737	80.02 ± 7.25
52360.0700	-125.61 ± 16.96	52390.2367	-22.02 ± 1.93	53095.1184	-45.75 ± 5.32	53303.7586	-1.28 ± 23.51
52360.0841	-109.78 ± 16.13	52390.9751	34.98 ± 2.38	53095.1395	-60.46 ± 6.21	53303.7719	12.97 ± 8.03

Table 9. Radial velocity measurements for the 28 sdB binaries which we present in this paper.

HMJD	RV (km s ⁻¹)	HMJD	RV (km s ⁻¹)	HMJD	RV (km s ⁻¹)	HMJD	RV (km s ⁻¹)
<u>EC20182-6534</u>		<u>EC20369-1804</u>		<u>EC21556-5552</u>		<u>EC22590-4819</u>	
53303.8700	68.48 ± 7.28	52893.9340	-6.77 ± 3.96	53655.9307	79.46 ± 6.34	52896.8993	54.81 ± 7.33
53303.8841	64.39 ± 7.20	52895.8477	-7.98 ± 9.60	53655.9414	62.31 ± 6.25	52896.9100	45.90 ± 14.20
53543.9901	49.05 ± 9.75	53300.8000	-40.33 ± 5.98	53656.8616	19.04 ± 5.09	52897.9100	67.73 ± 4.92
53544.0012	75.57 ± 16.40	53300.8108	-43.49 ± 6.39	53656.8723	22.31 ± 4.95	52897.9207	54.27 ± 5.96
53546.0133	11.16 ± 8.18	53301.8784	11.87 ± 5.51	53657.8573	-26.69 ± 6.93	53663.7933	53.59 ± 6.61
53546.0276	3.25 ± 7.47	53301.8891	12.50 ± 6.41	53657.8680	-22.73 ± 7.06	53663.8041	56.54 ± 6.54
53549.0111	-4.07 ± 7.40	53302.8296	53.09 ± 8.23	53658.8801	4.88 ± 12.27	<u>EC22590-4819</u>	
53549.0219	4.63 ± 7.17	53302.8403	61.51 ± 7.97	53658.8908	-2.28 ± 14.54	53664.8451	5.01 ± 7.54
53549.1810	-44.75 ± 7.76	53303.7928	18.90 ± 6.53	53659.8115	49.63 ± 6.43	53300.8525	58.12 ± 4.92
53654.8809	49.50 ± 8.83	53303.8035	22.68 ± 6.69	53659.8222	53.49 ± 5.10	53302.9837	45.65 ± 6.79
53654.8919	63.31 ± 11.29	53544.1446	-67.58 ± 23.49	53665.9305	68.31 ± 8.23	53302.9953	47.91 ± 8.37
53655.8991	19.20 ± 8.59	53544.1591	-67.34 ± 23.03	53663.7933	53.59 ± 6.61	53303.9058	19.18 ± 4.67
53655.9102	12.20 ± 8.59	53547.0553	60.74 ± 9.35	53663.8041	56.54 ± 6.54	53303.9165	18.58 ± 4.59
53656.7602	25.21 ± 6.00	53547.0698	40.14 ± 8.39	53664.8451	5.01 ± 7.54	53545.1258	-32.26 ± 4.78
53656.7710	14.87 ± 6.09	53656.8328	-50.54 ± 7.76	53666.9076	16.96 ± 5.67	53545.1365	-32.90 ± 5.41
<u>EC20260-4757</u>		53656.8435	-37.86 ± 8.38	53666.9186	-13.67 ± 5.88	53546.1411	-31.16 ± 10.75
52894.9204	65.63 ± 10.86	53659.8427	50.76 ± 8.39	<u>KPD2215+5037</u>		53546.1554	-28.23 ± 5.01
52894.9528	82.99 ± 16.01	53659.8534	44.36 ± 10.80	52183.1287	52.29 ± 2.76	53656.9639	-10.36 ± 10.23
52895.8292	89.89 ± 9.46	53663.7933	53.59 ± 6.61	52183.1357	42.32 ± 2.86	53656.9804	3.87 ± 6.32
52896.7817	114.17 ± 6.33	53663.8041	56.54 ± 6.54	52187.0800	79.97 ± 2.97	53657.9064	-24.32 ± 4.99
52896.7959	111.24 ± 6.78	53664.8451	5.01 ± 7.54	52187.0871	81.66 ± 2.95	53657.9171	-18.33 ± 4.96
52897.7588	90.95 ± 5.85	53664.8558	10.24 ± 7.69	52188.1216	-36.50 ± 2.96	53661.9111	38.85 ± 5.34
52897.7729	87.38 ± 5.96	53665.7515	-43.03 ± 6.44	52188.1287	-42.42 ± 3.10	53661.9254	15.74 ± 5.21
52897.9743	92.70 ± 14.57	<u>KPD2040+3955</u>		54330.1392	-82.78 ± 1.95	53666.9366	1.91 ± 6.15
52897.9885	77.23 ± 8.88	52184.0383	-60.06 ± 3.07	54330.1532	-83.14 ± 1.76	53666.9473	1.51 ± 6.29
52898.0010	78.52 ± 13.64	52184.0488	-55.54 ± 4.95	54331.8848	-20.74 ± 1.54	<u>PG2331+038</u>	
53300.7559	122.82 ± 9.00	52187.0305	-51.00 ± 3.00	54331.9023	-15.67 ± 1.45	52132.1785	-62.47 ± 4.68
53300.7797	121.78 ± 5.55	52187.0410	-42.91 ± 3.08	54333.1244	-15.83 ± 1.28	52132.1891	-61.35 ± 5.23
53301.8299	56.54 ± 5.09	52187.9203	-33.00 ± 2.53	54333.1419	-15.26 ± 1.36	52133.0754	-71.59 ± 3.43
53301.8526	45.62 ± 4.54	52187.9308	-34.74 ± 2.48	<u>EC22202-1834</u>		52133.0895	-77.34 ± 3.41
53302.8625	27.63 ± 6.75	52188.8410	67.40 ± 3.04	53544.1835	-71.66 ± 9.30	52187.1413	-3.65 ± 4.23
53302.8851	9.04 ± 5.16	52188.8515	74.17 ± 3.37	53545.0884	-71.74 ± 10.54	52187.1501	-4.18 ± 5.95
53303.8246	-6.66 ± 6.42	52189.0179	77.28 ± 3.18	53545.1056	-51.14 ± 7.73	54331.1209	-93.39 ± 3.26
53303.8472	-9.59 ± 6.20	52392.1846	80.69 ± 4.94	53546.1041	92.64 ± 8.46	54331.1419	-90.49 ± 4.08
53544.0935	31.44 ± 14.63	52393.1329	-61.16 ± 5.39	53546.1166	80.07 ± 21.73	54332.9926	75.74 ± 4.25
53544.1148	50.75 ± 13.41	52393.1470	-54.23 ± 5.21	53549.2076	-138.46 ± 14.68	54333.0136	62.61 ± 4.28
53546.0572	3.10 ± 4.72	54330.0499	48.10 ± 2.24	53656.9250	-84.10 ± 10.41	54333.1706	2.16 ± 2.61
53546.0785	10.30 ± 6.15	54330.0674	53.93 ± 2.07	53661.9477	-130.65 ± 11.82	54333.1915	-14.80 ± 2.70
53547.0094	28.71 ± 15.17	54331.9681	12.44 ± 3.18	53661.9620	-135.68 ± 13.25	54335.0123	3.08 ± 2.77
53547.0305	28.38 ± 9.84	54331.9856	11.53 ± 3.96	53663.9314	-41.10 ± 5.93	54335.0332	5.68 ± 2.57
53549.0464	101.67 ± 7.43	54332.8663	21.47 ± 9.37	53663.9456	-56.59 ± 6.07	54336.0388	-91.54 ± 2.63
53549.0675	96.19 ± 8.00	54332.8804	14.44 ± 6.10	53666.7486	-37.10 ± 5.84	54336.0597	-82.12 ± 2.84
53656.7914	105.77 ± 9.70	54334.1887	-67.00 ± 2.75	53666.7629	-39.40 ± 6.11	54338.0645	-42.37 ± 3.22
53656.8092	106.18 ± 7.70	54334.2062	-65.34 ± 2.85	53667.8629	64.20 ± 17.35	54338.0854	-46.50 ± 2.89
53658.8182	82.88 ± 5.21	<u>EC21556-5552</u>		<u>EC22590-4819</u>			
<u>EC20369-1804</u>		53654.9135	98.33 ± 15.59	52893.9488	-12.30 ± 2.65		
52893.9233	-5.02 ± 3.98	53654.9261	109.47 ± 16.25	52893.9595	-15.22 ± 2.69		

Table 10. Previously unpublished radial velocities for the remaining sdBs in our survey. Some of these show no significant variation. Others (which we mark with an asterisk) show signs of orbital variations but our data is insufficient to distinguish between competing aliases.

HMJD	RV (km s ⁻¹)	HMJD	RV (km s ⁻¹)	HMJD	RV (km s ⁻¹)	HMJD	RV (km s ⁻¹)
<u>EC00042-2737</u>		<u>EC00292-4741*</u>		<u>KPD0054+5406</u>		<u>EC03143-5945</u>	
53303.9894	33.51 ± 9.34	53658.0042	-8.25 ± 5.41	52132.1353	-37.95 ± 3.30	53659.0314	50.50 ± 8.85
53304.0040	30.00 ± 10.31	53658.8577	24.01 ± 7.21	52183.1818	-40.66 ± 2.45	<u>EC03238-0710</u>	
53547.1765	39.25 ± 8.63	53658.8649	12.75 ± 8.38	52183.1958	-39.09 ± 2.46	53300.0649	-10.38 ± 5.53
53657.9673	36.81 ± 11.90	53663.9137	16.72 ± 2.87	52184.1074	-27.10 ± 4.12	53300.0721	12.15 ± 5.62
53657.9815	45.64 ± 11.38	53665.7949	19.23 ± 4.01	52184.1215	-38.24 ± 3.12	53301.0418	-0.11 ± 4.88
53664.0050	34.68 ± 12.99	53665.8020	2.69 ± 3.97	<u>PG0057+155*</u>		53301.0490	-17.30 ± 5.46
53664.0207	3.85 ± 9.21	<u>PG0039+049</u>		52128.0948	18.80 ± 2.76	53301.0580	-5.30 ± 4.85
53665.0124	28.70 ± 3.85	52187.1957	-25.70 ± 1.69	52128.0984	14.44 ± 2.69	53301.0652	-12.13 ± 5.21
<u>PG0004+133</u>		52187.2028	-22.45 ± 1.83	52129.1504	29.83 ± 2.66	53302.0143	-6.86 ± 3.81
54332.2006	-0.58 ± 1.23	52188.1919	-29.51 ± 1.70	52129.1540	20.83 ± 2.69	53302.0215	-8.68 ± 3.91
54332.2181	-1.13 ± 1.21	52188.2005	-30.59 ± 1.76	52131.1173	30.29 ± 1.98	53302.0302	-19.03 ± 3.88
54335.2150	-9.53 ± 1.21	54330.2134	-25.92 ± 0.95	52131.1244	28.36 ± 2.03	53302.0374	-9.23 ± 3.86
54335.2290	-7.76 ± 1.17	54330.2274	-30.18 ± 0.98	52131.1505	28.17 ± 1.90	<u>EC03263-6403</u>	
54337.1654	0.41 ± 1.20	54332.0170	-31.86 ± 0.96	52131.1576	27.86 ± 1.89	53656.1026	5.54 ± 5.87
54337.1794	-1.81 ± 1.21	54332.0380	-31.27 ± 1.02	52181.1879	14.13 ± 1.86	53656.1167	11.80 ± 6.25
54342.2151	5.38 ± 1.83	54334.0766	-32.74 ± 1.03	52181.1950	21.15 ± 1.88	53657.0866	4.53 ± 6.81
54342.2291	1.61 ± 1.40	54334.0906	-34.42 ± 1.03	52182.2225	25.79 ± 1.39	53657.1008	1.88 ± 6.80
54342.2519	3.22 ± 2.59	54335.2150	-41.88 ± 1.45	52182.2296	26.21 ± 1.40	53658.0478	-14.19 ± 5.89
54343.0948	-8.68 ± 1.60	54338.1769	-35.40 ± 0.96	54330.2464	19.49 ± 1.02	53658.0620	-10.95 ± 5.86
54343.1089	-1.81 ± 1.26	54338.1944	-32.54 ± 0.87	54330.2604	9.10 ± 2.49	53658.9819	-11.39 ± 9.72
54343.1799	5.24 ± 1.22	<u>EC00405-3824*</u>		54331.2171	18.14 ± 1.35	53658.9960	-7.58 ± 6.35
54343.1940	-0.77 ± 1.15	52892.9688	-16.20 ± 1.96	54331.2346	18.10 ± 1.56	<u>EC03408-1315</u>	
54343.2136	-7.32 ± 1.13	52892.9726	-19.26 ± 2.00	54334.2371	14.59 ± 1.22	53665.0435	51.33 ± 5.87
54343.2276	-6.09 ± 1.16	52893.9722	-20.24 ± 1.67	54334.2511	11.76 ± 1.74	53665.0579	48.78 ± 5.87
54343.2437	-0.51 ± 1.12	52893.9759	-21.04 ± 1.80	54337.1289	18.55 ± 1.00	53666.0646	59.10 ± 7.11
<u>PG0005+179*</u>		53304.0194	-11.60 ± 2.55	54337.1430	17.58 ± 0.99	53666.0788	67.19 ± 7.01
52186.1804	-8.00 ± 5.55	53304.0236	-5.70 ± 2.51	54338.2184	13.94 ± 0.88	53667.0520	55.35 ± 6.84
52186.1926	3.00 ± 6.85	53304.0691	-6.39 ± 2.88	54338.2359	19.30 ± 0.92	53667.0661	64.68 ± 6.87
52188.1516	36.14 ± 3.95	53304.0730	-6.46 ± 3.12	<u>EC01120-5259</u>		<u>EC03470-5039</u>	
52188.1658	28.83 ± 4.07	53655.0267	-20.83 ± 3.41	52893.0184	62.72 ± 4.42	52893.0962	50.76 ± 4.74
54331.1744	-3.56 ± 4.02	53655.0305	-26.79 ± 7.69	52893.0327	64.52 ± 4.59	52893.1105	58.29 ± 4.72
54331.1919	-1.06 ± 4.53	53656.0326	-32.71 ± 2.66	52894.0373	68.34 ± 3.40	52894.1134	70.18 ± 3.84
54332.1551	-44.84 ± 5.43	53656.0364	-30.27 ± 2.74	52894.0514	63.31 ± 3.46	52897.0754	54.47 ± 6.08
54332.1726	-48.04 ± 5.02	53656.0401	-30.14 ± 2.73	53299.9896	64.83 ± 11.39	52897.0895	61.53 ± 5.38
54333.0405	-49.54 ± 3.57	53656.0439	-23.70 ± 2.71	53300.0062	67.72 ± 8.27	53300.0889	65.66 ± 6.41
54333.0580	-53.90 ± 3.57	53656.0476	-19.68 ± 2.65	<u>PB8783</u>		53300.1031	60.75 ± 6.31
54333.2292	-53.70 ± 5.90	53656.0514	-24.77 ± 2.64	52181.2185	12.02 ± 12.10	<u>EC03568-4849*</u>	
54333.2467	-50.77 ± 8.16	53656.8896	-22.51 ± 2.22	52181.2239	30.68 ± 10.57	52894.1485	35.95 ± 2.89
54334.0350	-10.59 ± 3.41	53656.8934	-22.89 ± 2.27	52181.2330	2.00 ± 21.92	52894.1626	25.64 ± 3.19
54334.0525	-15.38 ± 3.37	53656.8971	-19.25 ± 2.31	52182.2459	35.18 ± 2.68	52897.1078	24.03 ± 3.83
54342.0056	11.98 ± 6.40	53656.9008	-20.96 ± 2.12	52182.2496	28.81 ± 2.30	52897.1219	20.65 ± 3.69
54342.0231	3.56 ± 3.58	53656.9045	-20.45 ± 2.27	52184.2029	49.20 ± 10.38	53301.0832	11.60 ± 4.66
<u>EC00292-4741*</u>		53656.9083	-24.10 ± 2.20	52184.2065	27.63 ± 2.95	53301.0974	20.05 ± 4.80
52897.0353	-46.69 ± 3.19	53658.8425	-16.60 ± 2.32	<u>PB6710</u>		53302.0521	12.70 ± 4.13
52897.0425	-48.82 ± 3.04	53658.8463	-13.96 ± 2.90	52184.1752	36.06 ± 5.64	53302.0663	18.15 ± 4.07
52898.0735	-43.80 ± 2.84	<u>PG0046+207</u>		52184.1858	32.17 ± 2.70	53302.9138	24.43 ± 3.88
52898.0807	-47.07 ± 2.77	52133.1988	24.72 ± 3.85	<u>EC02542-3019</u>		53302.9281	20.65 ± 4.67
53303.9640	-5.79 ± 3.76	52133.2094	22.78 ± 3.78	53300.0305	17.86 ± 9.16	53664.0622	26.00 ± 7.31
53303.9713	-7.75 ± 3.77	52181.1641	21.29 ± 4.84	53300.0449	8.33 ± 8.89	<u>EC03591-3232*</u>	
53547.1945	-21.30 ± 13.40	52181.1746	19.02 ± 3.85	53301.0080	19.11 ± 5.52	52893.0734	45.97 ± 1.73
53547.2028	-33.12 ± 6.29	52182.1723	16.81 ± 3.21	53301.0236	3.92 ± 6.64	52893.0808	52.65 ± 1.76
53549.1554	-33.68 ± 4.24	52182.1829	26.43 ± 3.20	53301.9824	14.22 ± 5.82	52894.0908	59.72 ± 1.72
53549.1627	-39.53 ± 4.46	52183.2205	28.61 ± 3.77	53301.9967	6.32 ± 5.83	52894.0980	59.84 ± 1.70
53655.0063	-22.50 ± 6.64	52183.2311	26.73 ± 3.77	53664.0436	4.28 ± 6.09	52897.0535	49.87 ± 1.89
53655.0138	-21.55 ± 7.16	52186.2074	13.51 ± 4.77	<u>EC03143-5945</u>		52897.0607	59.91 ± 2.10
53655.9822	-10.64 ± 4.62	52186.2180	24.66 ± 4.62	53656.0679	37.54 ± 5.92	52898.1169	54.36 ± 1.68
53655.9894	-9.10 ± 4.78	<u>KPD0054+5406</u>		53656.0821	30.25 ± 5.39	52898.1241	57.47 ± 1.70
53655.9966	-12.94 ± 4.58	52129.1962	-31.91 ± 6.54	53657.0020	45.20 ± 5.28	53300.1243	55.19 ± 2.92
53656.0053	-22.42 ± 4.90	52129.2102	-29.05 ± 7.44	53657.0145	37.04 ± 7.82	53300.1316	56.59 ± 3.13
53656.0126	-11.99 ± 4.87	52130.2351	-38.25 ± 3.37	53657.0283	34.99 ± 4.86	<u>EC04170-3433</u>	
53656.0198	-17.10 ± 4.69	52130.2491	-37.14 ± 6.19	53659.0172	36.33 ± 7.34	53658.1013	68.22 ± 1.99

Table 10. Previously unpublished radial velocities for the remaining sdBs in our survey. Some of these show no significant variation. Others (which we mark with an asterisk) show signs of orbital variations but our data is insufficient to distinguish between competing aliases.

HMJD	RV (km s ⁻¹)	HMJD	RV (km s ⁻¹)	HMJD	RV (km s ⁻¹)	HMJD	RV (km s ⁻¹)
<u>EC04170-3433</u>		<u>PG0749+658</u>		<u>PG0749+658</u>		<u>PG0749+658</u>	
53658.1051	69.00 ± 1.90	51945.8625	-13.11 ± 1.31	52036.8594	-6.57 ± 2.84	54185.8518	-10.13 ± 2.91
53659.0714	68.94 ± 2.84	51976.8323	-8.10 ± 1.18	52036.8601	-8.38 ± 2.86	54190.8678	-18.49 ± 2.43
53659.0752	69.42 ± 2.90	51976.8358	-9.70 ± 1.13	52036.8608	-16.12 ± 2.85	54190.8701	-16.25 ± 2.51
53662.0616	71.37 ± 2.76	51977.8255	-15.65 ± 1.62	52036.8616	-5.13 ± 2.78	<u>PG0909+164</u>	
53662.0653	75.51 ± 3.12	51977.8291	-15.63 ± 1.48	52036.8623	-11.33 ± 2.86	52361.8937	51.79 ± 3.54
<u>EC04284-2758*</u>		51977.9144	-5.97 ± 1.43	52036.8630	-8.60 ± 2.71	52361.9043	52.41 ± 3.60
53666.1163	55.83 ± 4.75	51977.9179	-6.44 ± 1.48	52036.8637	-9.69 ± 2.61	52361.9456	53.86 ± 2.91
53666.1299	57.34 ± 6.53	51978.8258	-15.68 ± 1.67	52036.8645	-10.38 ± 2.57	52361.9561	56.12 ± 2.95
53667.0885	101.34 ± 6.32	51978.8293	-13.03 ± 1.26	52036.8652	-10.90 ± 2.56	52362.0358	48.40 ± 3.09
53667.1027	94.51 ± 6.26	51978.8621	-20.91 ± 2.32	52036.8659	-10.56 ± 2.50	52362.0463	42.13 ± 3.08
53668.0360	43.50 ± 12.84	51978.8628	-16.47 ± 2.33	52036.8666	-13.60 ± 2.67	52746.8660	61.94 ± 4.34
53668.0538	57.21 ± 8.94	51978.8636	-19.94 ± 2.38	52036.8674	-14.88 ± 2.61	52746.8778	55.77 ± 3.87
<u>EC04515-3754*</u>		51978.8643	-20.09 ± 2.37	52037.8514	-12.19 ± 5.43	54190.8904	57.18 ± 3.66
53659.0876	-11.95 ± 1.63	51978.8650	-16.35 ± 2.37	52037.8521	-11.70 ± 6.03	54190.9079	39.29 ± 2.90
53659.0948	-7.66 ± 1.68	51978.8709	-2.96 ± 2.95	52037.8528	-13.27 ± 4.98	54191.8710	36.02 ± 2.94
53662.0759	4.70 ± 2.25	51978.8716	-5.97 ± 2.28	52037.8535	-14.79 ± 4.89	54191.8850	43.32 ± 2.82
53662.0831	7.82 ± 2.13	51978.8723	-6.69 ± 2.29	52037.8542	-8.36 ± 4.97	54192.9597	40.19 ± 2.02
53664.1020	-17.43 ± 1.53	51978.8730	-6.21 ± 2.34	52037.8550	-6.45 ± 5.76	54192.9737	37.67 ± 2.17
53664.1092	-18.48 ± 1.62	51978.8738	-12.37 ± 2.32	52037.8557	-7.44 ± 3.52	54193.8615	36.94 ± 2.48
53665.1119	8.71 ± 3.94	51978.8745	-9.67 ± 2.33	52037.8564	-15.46 ± 4.07	54193.8755	39.06 ± 2.48
<u>EC04589-2945*</u>		51978.8752	-11.88 ± 2.27	52037.8571	-3.85 ± 4.25	54194.9249	46.26 ± 2.13
53301.1200	7.73 ± 5.14	51978.8760	-6.77 ± 2.35	52037.8578	-12.51 ± 3.62	54194.9389	42.53 ± 2.17
53302.0879	122.38 ± 5.25	51978.8767	-7.62 ± 2.36	52037.8585	0.82 ± 3.31	54903.9174	53.67 ± 2.16
53302.1020	110.70 ± 5.29	51978.8774	-14.89 ± 2.32	52037.8593	-8.66 ± 3.43	54903.9349	46.04 ± 2.05
53303.0538	4.65 ± 8.64	51978.8781	-5.72 ± 2.35	52037.8600	-2.61 ± 3.83	54906.0487	55.76 ± 2.26
53303.0679	0.66 ± 7.79	51978.8789	-8.03 ± 2.34	52037.8607	-12.89 ± 3.88	54906.0662	49.15 ± 2.50
53303.1195	9.66 ± 9.94	51978.8796	-5.91 ± 2.45	52037.8614	-8.28 ± 3.57	54906.8631	49.83 ± 2.47
53303.1303	48.93 ± 22.03	51978.8803	-10.16 ± 2.32	52037.8621	-0.22 ± 4.01	54906.8806	55.01 ± 2.28
53304.0385	96.75 ± 7.17	51978.8810	-11.88 ± 2.38	52037.8628	-5.12 ± 3.20	<u>PG0933+004</u>	
53304.0527	99.64 ± 7.33	51978.8818	-9.69 ± 2.35	52037.8636	-10.62 ± 3.54	52393.8731	53.92 ± 5.23
53304.0878	114.41 ± 8.94	51978.8825	-8.38 ± 2.32	52037.8643	-12.96 ± 3.27	52393.8838	55.14 ± 5.46
53304.1020	90.04 ± 8.90	51978.8832	-3.32 ± 2.46	52037.8650	-5.76 ± 3.80	52394.8762	53.96 ± 3.76
53304.1176	94.74 ± 8.58	51978.8840	-6.19 ± 2.33	52180.2424	-11.73 ± 4.18	52394.8868	51.16 ± 3.80
53655.1384	39.56 ± 23.78	51978.8847	-10.52 ± 2.32	52180.2439	1.97 ± 4.41	54189.9236	49.83 ± 3.08
53656.1385	92.46 ± 13.32	51978.9419	-14.48 ± 2.92	52738.9153	-13.75 ± 2.69	54189.9446	54.22 ± 3.27
53657.0519	30.03 ± 11.01	51978.9426	-15.67 ± 2.87	52738.9178	-10.18 ± 2.73	<u>EC09436-0929</u>	
53657.0661	-22.87 ± 10.94	51978.9433	-14.79 ± 2.80	52738.9204	-20.47 ± 2.48	52359.7877	-30.49 ± 29.16
53662.1226	88.52 ± 9.75	51978.9440	-9.91 ± 2.79	52738.9229	-11.42 ± 2.68	52362.8320	10.98 ± 6.02
53662.1350	78.45 ± 17.85	51978.9448	-18.03 ± 3.04	52738.9254	-11.95 ± 2.69	52362.8471	18.15 ± 6.38
53667.1319	116.74 ± 14.09	51978.9455	-8.95 ± 2.67	52738.9280	-14.30 ± 2.60	52363.8318	9.12 ± 7.90
53668.0949	-39.23 ± 12.13	51978.9462	-11.39 ± 3.23	52738.9305	-11.65 ± 2.47	52363.8459	14.37 ± 7.65
<u>EC05053-2806</u>		51978.9469	-10.45 ± 2.86	52738.9331	-7.65 ± 2.52	52719.8680	-6.47 ± 25.85
52893.1254	39.49 ± 1.87	51978.9477	-7.98 ± 3.04	52738.9356	-14.58 ± 2.41	52719.8841	-4.11 ± 17.56
52893.1328	35.48 ± 1.78	51978.9484	-1.80 ± 3.35	52738.9382	-19.18 ± 2.40	52719.9631	19.67 ± 15.59
52897.1362	31.81 ± 1.80	51978.9491	-12.39 ± 3.53	52738.9407	-11.65 ± 2.41	52719.9772	19.86 ± 15.29
52897.1434	29.87 ± 1.79	51978.9498	-7.92 ± 2.96	52738.9432	-12.20 ± 2.50	<u>EC10189-1502</u>	
53302.1254	35.25 ± 3.85	51978.9506	-6.33 ± 3.33	52738.9476	-19.25 ± 2.41	52359.8988	11.17 ± 18.76
53302.1293	36.10 ± 4.50	51978.9513	-3.72 ± 3.19	52738.9501	-19.21 ± 2.36	52359.9129	-11.31 ± 17.97
53302.1332	25.44 ± 6.56	51978.9520	-8.07 ± 3.30	52738.9526	-10.56 ± 2.47	52362.8943	-1.79 ± 6.36
53657.1205	25.59 ± 4.04	51978.9528	-2.13 ± 3.30	52738.9552	-16.28 ± 2.49	52362.9049	0.68 ± 6.21
<u>EC05479-5818</u>		51978.9535	-18.17 ± 3.34	52738.9577	-15.32 ± 2.51	52364.8087	-0.13 ± 4.38
53657.1350	5.25 ± 8.84	51978.9542	-12.85 ± 3.22	52738.9603	-13.27 ± 2.55	52364.8228	13.49 ± 4.14
53658.1184	6.35 ± 3.94	51978.9549	-9.48 ± 4.07	52738.9628	-14.51 ± 2.61	52719.8350	11.80 ± 10.61
53659.1094	11.94 ± 4.78	51978.9557	-7.72 ± 4.69	52738.9654	-17.14 ± 2.51	52719.8491	32.85 ± 11.59
53659.1236	13.98 ± 4.32	52036.8536	-6.88 ± 2.92	52738.9679	-15.62 ± 2.47	53094.9285	14.56 ± 9.72
53664.1324	16.10 ± 7.61	52036.8543	-10.08 ± 3.25	52738.9704	-16.31 ± 2.52	53094.9427	-14.05 ± 9.86
53665.1247	15.04 ± 3.35	52036.8550	-12.83 ± 3.03	52747.8432	-12.72 ± 3.17	53100.8440	-7.49 ± 7.77
<u>KPD0550+1922</u>		52036.8557	-11.48 ± 3.20	52747.8480	-6.44 ± 2.90	53100.8547	-12.56 ± 7.68
52188.2545	49.09 ± 3.39	52036.8565	-9.56 ± 3.22	54184.8605	-16.19 ± 3.70	53100.9694	4.77 ± 7.08
52188.2653	46.30 ± 3.65	52036.8572	-10.43 ± 3.36	54184.8680	-1.10 ± 2.99	53100.9836	11.55 ± 6.60
<u>PG0749+658</u>		52036.8579	-9.85 ± 2.83	54184.8702	0.23 ± 3.04	53101.8641	1.25 ± 11.79
51945.8583	-17.43 ± 1.34	52036.8587	-5.90 ± 3.05	54185.8496	-12.53 ± 3.26	53101.8748	-10.91 ± 11.85

Table 10. Previously unpublished radial velocities for the remaining sdBs in our survey. Some of these show no significant variation. Others (which we mark with an asterisk) show signs of orbital variations but our data is insufficient to distinguish between competing aliases.

HMJD	RV (km s ⁻¹)	HMJD	RV (km s ⁻¹)	HMJD	RV (km s ⁻¹)	HMJD	RV (km s ⁻¹)
<u>EC10189-1502</u>		<u>PG1040+234</u>		<u>EC12376-2049</u>		<u>PG1338+611</u>	
53101.8854	-27.59 ± 12.37	54906.0269	15.01 ± 1.53	53545.7824	30.32 ± 11.96	54195.2702	44.56 ± 1.94
53101.8961	-19.20 ± 12.14	54906.9538	13.33 ± 1.42	53548.7453	43.27 ± 11.97	54195.2745	-10.14 ± 3.71
53101.9085	4.20 ± 12.26	54906.9713	10.77 ± 1.40	53548.7597	57.06 ± 12.35	54195.8929	42.56 ± 0.88
53101.9192	16.63 ± 12.05	<u>PG1047+003</u>		<u>EC12473-3046</u>		54195.9035	43.86 ± 0.87
53101.9298	8.18 ± 12.43	51976.9999	-11.38 ± 3.48	53545.8062	76.64 ± 6.42	54196.9553	45.27 ± 1.26
53101.9405	10.12 ± 12.84	52032.9460	-17.75 ± 3.66	53545.8190	78.94 ± 8.34	54196.9596	44.28 ± 1.26
53102.8639	10.78 ± 5.01	52034.0248	-2.87 ± 3.31	53548.7846	61.74 ± 11.71	54197.0416	47.82 ± 1.29
53102.8957	9.45 ± 5.14	52036.0172	-13.94 ± 15.71	53548.8222	81.27 ± 6.57	54197.0459	49.03 ± 1.35
53102.9167	-3.71 ± 4.88	52037.0033	-3.46 ± 2.88	<u>EC12578-2107</u>		54197.1015	37.64 ± 1.21
<u>PG1039+219</u>		52037.9337	-8.28 ± 4.02	53545.8756	15.57 ± 5.73	54197.1058	38.45 ± 1.27
51946.0203	-8.70 ± 2.67	52747.9020	-0.90 ± 3.99	53545.8863	21.37 ± 5.24	54197.2035	56.45 ± 1.92
52034.0477	0.00 ± 1.75	52747.9162	-12.74 ± 4.55	53548.8443	29.01 ± 9.09	54197.2078	52.63 ± 2.23
52037.0255	3.60 ± 1.43	<u>PG1114+073</u>		53548.8585	34.86 ± 9.43	54197.2139	35.03 ± 1.79
52744.9412	-3.01 ± 2.54	51977.0449	6.77 ± 1.82	<u>PG1303+097*</u>		54197.2182	37.96 ± 1.41
52744.9518	-4.37 ± 2.74	52036.0000	8.66 ± 6.17	51947.2161	13.64 ± 7.09	54197.2243	40.87 ± 1.49
54185.9767	-11.09 ± 2.01	52037.0554	10.42 ± 1.97	52036.1124	36.62 ± 2.51	54197.2286	40.63 ± 1.61
54185.9907	-9.77 ± 2.21	52746.9549	6.51 ± 2.21	52037.1135	31.53 ± 4.58	54197.2348	44.32 ± 1.88
54187.9545	-12.98 ± 2.03	52746.9643	12.70 ± 2.22	52037.1239	30.91 ± 4.98	54197.2391	44.23 ± 1.52
54187.9685	-7.65 ± 1.84	54190.9821	-1.38 ± 1.51	52038.0807	24.62 ± 5.85	<u>PG1352-023</u>	
54189.0415	-25.45 ± 2.12	54190.9996	5.20 ± 1.82	52038.0911	25.70 ± 7.14	52390.1508	-15.35 ± 16.82
54189.0555	-24.43 ± 2.20	54191.9809	3.31 ± 2.23	52038.1021	27.20 ± 7.76	52390.1614	-19.49 ± 4.31
54191.9094	-13.80 ± 1.83	54191.9949	6.42 ± 2.06	52038.1121	31.39 ± 11.22	52392.0517	-29.03 ± 2.87
54191.9235	-13.90 ± 1.91	54195.8622	7.45 ± 2.11	52747.9370	42.67 ± 5.05	52392.0555	-35.64 ± 2.94
54196.8956	-1.73 ± 1.95	54195.8727	7.51 ± 1.65	52747.9495	40.39 ± 14.02	52394.9210	-27.27 ± 2.16
54196.9096	-3.02 ± 1.82	<u>PG1130+054</u>		54193.0802	26.92 ± 2.63	52394.9282	-26.79 ± 2.11
54197.1287	-8.49 ± 2.50	52361.9977	8.88 ± 4.62	54193.1012	28.83 ± 2.42	54193.0571	-23.25 ± 2.53
54197.1442	-4.93 ± 2.43	52362.0186	14.52 ± 4.68	54545.0140	26.51 ± 3.61	54193.0614	-24.50 ± 2.55
54546.9769	-10.46 ± 1.52	52362.1173	4.49 ± 4.41	54545.0316	24.07 ± 3.91	54544.2270	-33.23 ± 1.60
54546.9910	-11.16 ± 1.66	52362.1383	4.07 ± 5.35	54906.1754	28.73 ± 4.13	54544.2410	-33.30 ± 1.63
54905.8823	-1.46 ± 1.19	54193.0000	-7.02 ± 2.89	54906.1964	30.86 ± 3.68	<u>PG1407-013</u>	
54905.9033	-1.99 ± 1.13	54193.0210	-5.92 ± 2.98	<u>EC13047-3049</u>		52360.0276	-102.30 ± 15.44
54905.9776	-0.24 ± 1.61	54547.0490	-5.34 ± 4.89	52359.9971	16.42 ± 7.55	52360.0417	-133.41 ± 15.08
54905.9917	-0.23 ± 1.62	54547.0665	-9.37 ± 4.57	52360.0077	40.11 ± 7.63	52362.0156	-98.83 ± 26.56
<u>PG1040+234</u>		54907.0693	11.60 ± 3.19	52361.9625	13.41 ± 6.54	52362.0297	-67.10 ± 25.02
51946.0367	6.35 ± 3.15	54907.0903	14.44 ± 3.08	52361.9766	17.91 ± 6.77	52362.9685	-113.62 ± 8.41
52037.0432	14.40 ± 1.92	<u>EC11349-2753</u>		52362.9420	39.87 ± 3.57	52362.9792	-92.02 ± 8.26
52037.8874	3.49 ± 8.32	52361.8984	-14.89 ± 12.15	52362.9526	27.28 ± 3.62	52364.0652	-126.35 ± 19.27
52746.8968	4.46 ± 2.47	52361.9108	-19.36 ± 20.49	52362.9945	30.40 ± 3.48	52364.0793	-104.82 ± 19.08
52746.9074	8.37 ± 2.45	52361.9286	-15.34 ± 8.40	52363.0056	29.88 ± 3.64	52365.0581	-99.49 ± 5.03
52747.8675	10.43 ± 3.09	52361.9427	-37.76 ± 10.82	52364.0365	25.37 ± 5.83	52720.0301	-89.97 ± 8.17
52747.8817	14.39 ± 2.71	52362.9197	-30.06 ± 4.54	52364.0471	42.75 ± 5.74	52720.0442	-93.80 ± 8.17
54190.9385	-3.17 ± 1.67	52362.9268	-18.69 ± 4.44	52364.0982	23.95 ± 6.20	53100.8787	-87.25 ± 5.11
54190.9595	-0.05 ± 1.53	52364.9228	-29.81 ± 3.34	52364.1123	31.33 ± 7.17	53100.8997	-96.51 ± 5.31
54193.8964	-3.54 ± 1.37	52364.9317	-21.52 ± 2.66	52364.9466	31.38 ± 3.08	53101.0302	-122.19 ± 15.09
54193.9104	-5.89 ± 1.36	<u>EC12234-2607</u>		52364.9561	31.68 ± 3.10	53101.0582	-119.39 ± 12.12
54194.1416	19.04 ± 1.49	52719.9348	11.68 ± 13.39	<u>PG1338+611</u>		53101.0770	-86.12 ± 12.54
54194.1614	19.48 ± 1.70	52719.9454	38.80 ± 14.30	52390.0343	45.09 ± 2.18	53106.0067	-70.69 ± 12.19
54194.8916	1.72 ± 1.56	52720.9674	69.91 ± 20.67	52390.0415	44.04 ± 1.57	53106.0226	-114.10 ± 12.11
54194.9056	3.17 ± 1.56	52720.9816	4.82 ± 23.17	52390.1246	41.56 ± 2.25	53107.0461	-95.84 ± 10.85
54195.9713	5.41 ± 2.21	53107.0207	39.23 ± 7.41	52390.1318	39.38 ± 2.43	53107.0629	-93.61 ± 6.81
54195.9888	0.03 ± 1.68	53107.0279	28.17 ± 7.26	52392.1058	50.62 ± 2.26	53107.9971	-103.22 ± 13.01
54196.9290	-9.18 ± 1.95	53545.7403	35.39 ± 7.25	52392.1095	45.83 ± 2.32	53108.0113	-92.68 ± 13.06
54196.9430	-9.40 ± 1.88	53545.7512	21.83 ± 7.68	54190.0094	55.29 ± 1.32	54196.0987	-90.86 ± 2.17
54547.0116	0.06 ± 1.66	53548.8794	53.19 ± 19.67	54190.0137	56.90 ± 1.37	54196.1197	-93.53 ± 2.01
54547.0257	0.55 ± 1.74	<u>PG1237+132</u>		54191.1378	48.63 ± 1.21	54548.0888	-102.22 ± 2.43
54553.0278	4.63 ± 3.49	51977.0647	-41.22 ± 5.71	54191.1421	49.12 ± 1.24	54548.1075	-101.78 ± 2.23
54553.0488	2.49 ± 2.86	52035.1142	-30.62 ± 16.03	54193.0359	21.38 ± 1.26	<u>PG1417+257</u>	
54900.9771	5.91 ± 3.75	52038.0505	-40.43 ± 5.17	54193.0402	26.23 ± 1.26	51946.1830	-4.89 ± 1.52
54900.9980	10.70 ± 5.63	52740.0331	-40.28 ± 4.82	54194.0897	38.90 ± 1.23	52035.1598	2.38 ± 1.33
54904.0020	5.15 ± 1.53	52740.0473	-36.84 ± 4.83	54194.0940	38.11 ± 1.29	52036.1559	-3.54 ± 1.45
54904.0160	11.86 ± 2.42	<u>EC12376-2049</u>		54195.2597	49.68 ± 1.29	52037.1378	0.24 ± 2.02
54906.0129	2.74 ± 1.59	53545.7696	26.70 ± 20.04	54195.2640	49.20 ± 1.41	52393.0428	5.72 ± 2.11

Table 10. Previously unpublished radial velocities for the remaining sdBs in our survey. Some of these show no significant variation. Others (which we mark with an asterisk) show signs of orbital variations but our data is insufficient to distinguish between competing aliases.

HMJD	RV (km s ⁻¹)	HMJD	RV (km s ⁻¹)	HMJD	RV (km s ⁻¹)	HMJD	RV (km s ⁻¹)
PG1417+257		PG1432+004		PG1526+132*		PG1610+519*	
52393.0569	-5.14 ± 2.05	52361.1965	-0.79 ± 1.62	52362.1744	5.54 ± 4.88	52187.8507	-19.15 ± 2.39
52393.0927	-7.77 ± 2.50	52362.1548	2.35 ± 1.99	52362.1884	11.92 ± 4.71	52748.0400	13.59 ± 5.00
52393.1033	-9.47 ± 2.55	52362.1619	0.88 ± 1.91	52362.2296	3.83 ± 2.98	52748.0541	10.02 ± 4.30
52739.0635	0.05 ± 3.16	52363.2310	2.15 ± 3.69	52362.2436	2.98 ± 2.64	52748.1636	3.96 ± 4.82
52739.0742	-3.81 ± 3.17	52363.2418	1.52 ± 3.60	54190.1838	10.59 ± 3.03	52748.1777	6.03 ± 5.68
52740.0645	-4.30 ± 3.30	54190.1638	-10.27 ± 1.95	54190.2013	9.56 ± 2.19	54545.1323	-48.00 ± 1.94
52740.0751	-8.59 ± 2.94	54190.1686	-10.57 ± 1.77	54547.2543	-21.03 ± 2.82	54545.1498	-54.29 ± 1.85
52744.9922	-6.57 ± 3.10	54195.1515	-9.65 ± 1.27	54547.2718	-17.36 ± 3.31	54548.1723	-27.30 ± 2.46
52745.0063	-2.27 ± 3.15	54195.1621	-14.30 ± 1.35	54550.1673	-23.96 ± 4.18	54548.1863	-31.18 ± 2.55
52746.9255	-2.33 ± 2.74	EC14338-1445		54550.1883	-26.23 ± 3.43	54548.2444	-25.75 ± 2.63
52746.9361	-2.33 ± 2.72	53544.8879	-5.10 ± 7.91	54902.2460	-24.95 ± 4.52	54548.2585	-27.13 ± 3.83
52747.0070	0.33 ± 3.10	53544.8987	-5.64 ± 7.71	54902.2635	-29.73 ± 3.86	54548.2771	-31.90 ± 5.12
52747.0177	-7.27 ± 3.24	53546.9062	-8.69 ± 8.07	54905.1413	-20.86 ± 3.10	54550.2163	-19.66 ± 2.55
52747.0299	-4.46 ± 2.91	53546.9171	3.16 ± 11.42	54905.1588	-20.84 ± 2.98	54550.2304	-28.99 ± 2.95
52747.0406	3.66 ± 2.83	53548.9379	-4.83 ± 7.65	54906.2167	-19.43 ± 5.67	54550.2516	-11.43 ± 6.60
52748.1072	4.06 ± 3.37	53548.9521	2.23 ± 9.12	54906.2296	-25.11 ± 2.95	54904.2263	15.10 ± 2.59
52748.1190	-7.04 ± 3.20	EC14345-1729		54907.1137	-28.27 ± 4.69	54904.2404	3.17 ± 4.21
54188.1826	-9.50 ± 2.41	52362.0482	-43.26 ± 5.76	54907.1312	-20.77 ± 3.45	54907.1931	7.75 ± 2.39
54188.1967	-10.24 ± 2.26	52362.0623	-48.58 ± 5.86	54952.0473	10.14 ± 5.08	54907.2071	10.11 ± 2.63
54189.0800	-0.22 ± 1.96	53101.1005	-35.71 ± 2.80	54952.0718	7.20 ± 2.99	54951.2348	7.67 ± 2.41
54189.0941	-1.89 ± 1.93	53101.1216	-42.55 ± 2.76	54952.0812	7.45 ± 2.83	54951.2384	13.13 ± 2.35
EC14230-2231*		53106.0465	-39.98 ± 3.79	PG1548+166		54951.2421	14.19 ± 2.35
52719.0668	-39.76 ± 13.13	53106.0609	-34.66 ± 3.57	52361.2562	28.70 ± 7.87	54952.1257	1.00 ± 4.79
52719.0757	-94.12 ± 21.77	53107.0920	-37.21 ± 4.63	52361.2668	18.21 ± 8.04	54952.1397	19.07 ± 2.97
52719.1305	-150.89 ± 37.20	53108.0331	-41.43 ± 6.80	52362.2036	40.88 ± 8.38	54952.1561	4.37 ± 1.75
52719.1605	-110.01 ± 10.40	53108.0475	-45.39 ± 7.24	52362.2141	28.51 ± 7.70	54952.1672	4.66 ± 1.51
52719.1713	-116.13 ± 14.93	PG1438+018		52394.0486	24.17 ± 7.03	52748.0400	13.09 ± 5.14
52720.0872	-79.22 ± 12.90	52361.1455	-45.37 ± 4.30	52394.0558	15.91 ± 6.97	52748.0541	11.17 ± 4.42
52720.0978	-75.43 ± 11.82	52361.1664	-33.97 ± 3.84	54193.1963	8.76 ± 2.81	52748.1636	5.12 ± 4.97
53544.8563	-49.73 ± 37.12	52362.0812	-33.31 ± 4.06	54193.2173	6.67 ± 2.97	52748.1777	6.05 ± 5.86
53544.8688	-96.54 ± 28.14	52362.0953	-43.65 ± 3.74	54194.2572	25.92 ± 3.53	PG1616+144	
53546.8747	69.49 ± 23.11	52393.9766	-36.82 ± 3.75	54194.2712	2.04 ± 6.38	51946.2296	-51.18 ± 3.14
53546.8857	85.91 ± 16.48	52393.9873	-40.60 ± 3.61	54195.0366	25.52 ± 5.23	52034.1993	-45.63 ± 5.24
53548.9025	-98.24 ± 19.60	54545.0455	-49.10 ± 3.32	54195.0541	19.29 ± 3.92	52035.2351	-52.79 ± 8.30
53548.9167	-137.91 ± 20.44	54545.0630	-50.38 ± 2.91	54196.2038	5.13 ± 3.10	52036.1726	-40.06 ± 2.69
PG1424+332		PG1505+074		54196.2247	-3.98 ± 2.97	52037.1736	-47.34 ± 2.84
52393.9187	5.09 ± 3.32	52391.1418	-0.73 ± 6.84	54197.1688	-2.45 ± 5.50	52038.2216	-53.54 ± 4.66
52393.9293	8.39 ± 2.99	52391.1490	6.31 ± 4.56	54197.1863	-6.28 ± 6.38	PG1618+563	
52395.0335	3.39 ± 2.80	52395.1176	2.82 ± 3.45	54548.2104	12.93 ± 5.23	54545.1772	-77.62 ± 0.60
52395.0442	12.31 ± 2.87	52395.1214	4.76 ± 3.69	54548.2244	-1.35 ± 5.43	54545.1912	-78.39 ± 0.62
54193.1325	18.04 ± 2.79	52395.2391	3.82 ± 6.14	PG1551+256		PG1627+112	
54193.1465	22.35 ± 2.99	52395.2428	-1.43 ± 7.56	52394.0691	-66.29 ± 2.27	52362.2618	-12.48 ± 3.90
54547.2183	-4.24 ± 2.30	54193.1624	12.45 ± 2.47	52394.0812	-62.77 ± 2.31	52362.2758	-8.23 ± 10.79
54547.2323	-0.96 ± 2.30	54193.1668	-2.13 ± 2.47	54191.1605	-64.05 ± 1.51	54190.2332	-16.48 ± 2.53
54548.1312	10.80 ± 2.64	54195.2238	-5.08 ± 2.70	54191.1815	-66.25 ± 1.70	54190.2507	-18.59 ± 2.54
54548.1487	2.05 ± 2.53	54195.2274	0.61 ± 2.74	PG1553+273		HD149382	
54553.1802	9.54 ± 3.72	EC15103-1557		52392.0787	71.91 ± 2.10	52361.2778	27.94 ± 0.84
54553.2016	10.65 ± 2.56	52360.1200	19.99 ± 4.45	52392.0859	71.49 ± 2.04	52361.2800	34.51 ± 0.83
54553.2173	3.66 ± 2.68	52360.1364	36.32 ± 4.81	54545.0865	72.96 ± 1.37	52361.2822	33.43 ± 0.83
54553.2336	4.28 ± 2.76	52362.1020	1.65 ± 10.20	54545.1005	74.15 ± 1.41	52362.1591	11.59 ± 0.98
54553.2476	5.18 ± 3.34	52362.1161	34.77 ± 11.51	PG1610+519*		52362.1651	13.63 ± 0.94
54553.2637	1.48 ± 4.24	52362.1317	47.53 ± 17.09	52130.8838	-20.02 ± 3.37	52362.1711	12.55 ± 0.96
54902.0890	16.40 ± 3.20	52362.1458	24.47 ± 20.53	52130.8944	-22.54 ± 3.30	52362.2884	28.65 ± 1.82
54902.1134	13.60 ± 2.80	52363.0728	28.63 ± 3.66	52130.9398	-21.51 ± 3.40	52362.2906	28.45 ± 2.30
54904.2657	10.22 ± 2.92	52363.0834	20.84 ± 3.74	52130.9503	-18.88 ± 3.48	52363.1524	21.11 ± 1.17
54904.2798	10.54 ± 4.15	52363.1320	37.71 ± 4.56	52131.8650	-13.13 ± 3.38	52363.1549	21.56 ± 1.17
54905.1843	18.84 ± 2.49	52363.1426	33.72 ± 4.68	52131.8756	-17.00 ± 3.10	52363.1574	20.08 ± 1.13
54905.2018	18.15 ± 2.71	52364.1312	29.68 ± 6.69	52182.8379	-22.18 ± 2.60	52363.1599	20.59 ± 1.11
PG1432+004		52364.1453	18.70 ± 6.34	52182.8484	-25.55 ± 2.61	52363.1624	19.70 ± 1.18
52361.0837	3.43 ± 1.85	PG1526+132*		52186.8947	-17.24 ± 3.23	52363.1650	21.15 ± 1.18
52361.0943	-0.11 ± 1.95	52361.2161	15.10 ± 3.94	52186.9052	-17.83 ± 3.38	52363.1675	18.92 ± 1.18
52361.1860	1.22 ± 1.68	52361.2371	19.85 ± 3.73	52187.8401	-15.52 ± 2.68	52363.1700	20.26 ± 1.22

Table 10. Previously unpublished radial velocities for the remaining sdBs in our survey. Some of these show no significant variation. Others (which we mark with an asterisk) show signs of orbital variations but our data is insufficient to distinguish between competing aliases.

HMJD	RV (km s ⁻¹)	HMJD	RV (km s ⁻¹)	HMJD	RV (km s ⁻¹)	HMJD	RV (km s ⁻¹)
<u>HD149382</u>		<u>HD149382</u>		<u>PG1701+359</u>		<u>KPD1924+2932</u>	
52364.1566	17.98 ± 1.63	52393.0285	32.03 ± 1.27	54188.2578	-120.96 ± 1.88	52183.9450	57.44 ± 2.98
52364.1591	17.84 ± 1.76	52393.0301	32.59 ± 1.27	54188.2722	-125.33 ± 3.68	52183.9521	60.81 ± 3.63
52364.1616	17.55 ± 1.74	52393.0318	29.37 ± 1.23	54189.1522	-124.95 ± 1.31	52186.0000	45.92 ± 4.91
52364.1642	17.58 ± 1.64	52739.2503	24.72 ± 0.93	54189.1662	-123.32 ± 1.29	52186.0071	62.25 ± 4.66
52364.1667	19.34 ± 1.60	52739.2523	22.69 ± 1.09	54330.1793	-114.28 ± 1.16	52186.9886	51.84 ± 3.31
52364.1692	20.75 ± 1.61	52739.2543	25.59 ± 1.01	54330.8831	-118.61 ± 2.02	52186.9957	54.53 ± 3.29
52364.1717	19.40 ± 1.63	52739.2562	24.86 ± 1.59	54330.8971	-118.75 ± 2.09	<u>EC19563-7205</u>	
52364.1743	21.29 ± 1.63	52739.2582	24.29 ± 1.95	<u>PG1710+490</u>		52896.8707	-19.77 ± 8.20
52364.1789	18.08 ± 1.63	52739.2601	24.81 ± 0.92	51946.2434	-53.09 ± 2.88	52896.8814	-38.25 ± 8.64
52365.1593	18.47 ± 1.08	52739.2621	24.15 ± 0.95	52034.2389	-52.94 ± 2.31	52897.8471	-22.23 ± 4.76
52365.1619	16.24 ± 1.08	52739.2641	25.18 ± 0.95	52034.2429	-49.39 ± 2.34	52897.8578	-6.61 ± 12.61
52365.1644	16.36 ± 1.07	52739.2660	25.90 ± 0.93	52034.2472	-49.02 ± 2.77	53545.9798	-19.00 ± 5.24
52365.1669	18.69 ± 1.07	54190.2750	27.12 ± 0.75	52037.1822	-46.53 ± 2.68	53545.9907	-24.19 ± 6.78
52365.1695	17.20 ± 1.08	54190.2764	21.93 ± 0.84	52037.1863	-49.21 ± 2.38	<u>EC19590-5200*</u>	
52365.1720	18.82 ± 1.11	54190.2795	16.02 ± 0.87	52182.8816	-43.41 ± 2.29	52892.7990	45.36 ± 5.88
52365.1745	17.37 ± 1.11	54190.2807	10.77 ± 1.19	52182.8852	-42.20 ± 2.27	52892.8133	45.88 ± 7.79
52365.1770	16.61 ± 1.12	54193.2774	25.00 ± 0.86	54189.2701	-56.66 ± 2.78	52893.7880	73.26 ± 4.82
52365.1795	18.25 ± 1.15	54193.2796	20.47 ± 1.19	54189.2744	-59.96 ± 3.81	52893.8021	75.26 ± 5.02
52388.1977	28.23 ± 1.19	54195.1342	26.27 ± 0.63	54191.2502	-49.80 ± 2.66	52895.7961	93.76 ± 5.76
52388.2049	28.54 ± 1.28	54195.1364	15.17 ± 0.80	54191.2546	-45.17 ± 2.54	52895.8103	108.31 ± 6.85
52390.2096	29.96 ± 0.53	<u>PG1632+088</u>		54192.2629	-55.55 ± 2.03	52896.7289	128.92 ± 6.69
52390.2151	29.15 ± 0.72	54191.2158	192.13 ± 1.08	54192.2699	-63.24 ± 2.43	52896.7431	139.23 ± 5.58
52391.0803	27.29 ± 0.99	54191.2299	192.38 ± 1.06	54329.9335	-52.79 ± 1.04	52897.7257	136.12 ± 11.80
52391.0852	29.01 ± 0.86	<u>PG1644+404</u>		54329.9475	-49.82 ± 1.07	52897.7398	142.07 ± 10.39
52391.2427	27.91 ± 0.75	52394.1401	101.30 ± 2.70	54330.9186	-49.02 ± 1.44	52897.8775	140.92 ± 6.28
52391.2452	28.63 ± 0.75	52394.1543	105.51 ± 2.61	54330.9326	-47.47 ± 1.26	52897.8917	129.12 ± 6.49
52391.2478	27.29 ± 0.75	<u>PG1647+056</u>		<u>PG1722+286</u>		53101.1429	130.66 ± 5.28
52391.2504	27.76 ± 0.75	54193.2328	-104.43 ± 4.42	51977.2826	-27.17 ± 5.13	53101.1535	133.69 ± 5.46
52391.2529	28.28 ± 0.72	54193.2468	-108.35 ± 3.83	52034.1478	-37.34 ± 3.04	53103.0905	83.36 ± 6.29
52391.2555	27.82 ± 0.85	<u>PG1653+131*</u>		52036.2187	-28.65 ± 2.67	53103.1116	86.01 ± 6.55
52391.2581	29.10 ± 0.77	51982.2496	-2.01 ± 2.87	52037.2022	-61.98 ± 14.84	53107.1759	37.01 ± 12.54
52391.2606	27.10 ± 0.88	52033.1066	7.19 ± 2.49	52037.2036	-47.45 ± 14.96	53108.1298	76.15 ± 5.34
52391.2632	27.02 ± 1.39	52033.2337	4.08 ± 4.54	52037.2051	-25.80 ± 12.12	53108.1441	86.95 ± 5.38
52392.0604	28.69 ± 1.09	52035.2185	19.11 ± 5.86	52037.2065	-35.08 ± 11.64	53544.0492	46.37 ± 10.03
52392.0621	28.94 ± 1.05	52036.2051	9.42 ± 2.53	52037.2079	-45.74 ± 11.40	53544.0638	37.60 ± 10.60
52392.0637	29.53 ± 1.03	52038.1974	-2.01 ± 8.94	52037.2093	-34.92 ± 12.08	53546.9695	107.55 ± 14.66
52392.0654	29.92 ± 1.06	52038.2374	-0.29 ± 11.04	52037.2108	-46.19 ± 12.35	53546.9839	77.38 ± 9.78
52392.0670	29.45 ± 1.00	52128.9253	14.55 ± 3.83	52037.2438	-33.01 ± 5.20	53654.8354	81.81 ± 12.05
52392.0686	30.41 ± 1.04	52183.8515	25.23 ± 3.08	52127.9496	-36.25 ± 3.47	53654.8535	77.72 ± 10.12
52392.0703	28.88 ± 1.02	52187.8222	8.60 ± 3.12	52183.8874	-29.44 ± 2.42	53655.7609	63.34 ± 40.06
52392.0719	26.79 ± 1.05	52745.0815	-3.75 ± 3.45	54191.2680	-40.09 ± 4.42	53655.7827	55.50 ± 7.47
52392.2390	29.64 ± 1.07	52745.0957	-3.47 ± 3.35	54191.2723	-37.86 ± 6.28	53663.7399	152.14 ± 6.42
52392.2406	31.72 ± 1.05	52746.1484	4.56 ± 5.20	54195.2350	-26.41 ± 3.34	53665.7720	108.22 ± 5.81
52392.2422	31.27 ± 1.05	52747.0566	3.99 ± 4.65	54195.2407	-35.07 ± 2.46	53665.8170	105.95 ± 6.34
52392.2439	28.44 ± 1.06	52747.0707	8.55 ± 5.78	54329.9704	-40.33 ± 1.59	53665.8312	117.84 ± 6.46
52392.2455	31.02 ± 1.09	52747.1440	3.10 ± 5.49	54329.9844	-38.79 ± 1.55	<u>EC20106-5248</u>	
52392.2472	27.78 ± 1.09	52747.1582	-1.76 ± 4.59	54330.9545	-36.64 ± 2.28	52892.8308	-6.54 ± 2.78
52392.2488	29.71 ± 1.10	54189.2403	-4.62 ± 2.57	54330.9685	-34.13 ± 2.43	52892.8416	-7.85 ± 2.71
52392.2504	28.11 ± 1.12	54189.2544	-7.62 ± 2.44	<u>KPD1901+1607</u>		52893.8187	-6.24 ± 2.15
52392.2521	29.02 ± 1.13	54905.1413	3.05 ± 2.64	52127.9893	-3.17 ± 4.07	52893.8293	-8.25 ± 2.17
52392.2537	31.02 ± 1.13	<u>PG1701+359</u>		52128.0033	-7.49 ± 3.89	53103.1507	-7.42 ± 2.50
52392.2565	30.18 ± 1.15	52034.2152	-120.30 ± 1.82	52128.1132	-9.46 ± 4.20	53106.1580	-2.39 ± 3.03
52392.2581	28.18 ± 1.17	52036.2293	-119.97 ± 1.61	52128.1272	-6.22 ± 4.43	53106.1652	-7.63 ± 3.00
52392.2597	24.59 ± 1.36	52037.1958	-112.88 ± 2.26	52128.9454	-0.56 ± 3.56	<u>EC20117-4014</u>	
52392.2614	25.15 ± 1.56	52182.8693	-104.66 ± 2.86	52128.9594	-0.43 ± 3.72	52892.9112	16.67 ± 2.46
52393.0170	30.41 ± 1.37	52182.8729	-101.96 ± 2.84	52129.9167	-1.54 ± 3.35	52892.9221	19.47 ± 2.75
52393.0187	30.84 ± 1.32	52183.8352	-123.06 ± 3.18	52129.9307	-2.47 ± 3.31	52893.8960	19.14 ± 1.91
52393.0203	31.50 ± 1.37	52183.8388	-120.89 ± 3.96	52132.8760	0.50 ± 4.80	52893.9067	19.59 ± 1.95
52393.0220	29.95 ± 1.33	52187.9003	-107.47 ± 3.04	52132.8866	-0.91 ± 4.14	53114.1514	18.44 ± 2.96
52393.0236	31.91 ± 1.33	52187.9039	-111.87 ± 2.98	52186.9329	-2.62 ± 3.39	53114.1756	18.34 ± 3.00
52393.0252	30.10 ± 1.32	52744.2323	-117.27 ± 2.66	52186.9469	1.19 ± 3.55	53657.8148	0.53 ± 11.50
52393.0269	32.72 ± 1.28	52744.2429	-117.32 ± 2.71			53657.8276	17.51 ± 2.80

Table 10. Previously unpublished radial velocities for the remaining sdBs in our survey. Some of these show no significant variation. Others (which we mark with an asterisk) show signs of orbital variations but our data is insufficient to distinguish between competing aliases.

HMJD	RV (km s ⁻¹)	HMJD	RV (km s ⁻¹)	HMJD	RV (km s ⁻¹)	HMJD	RV (km s ⁻¹)
<u>EC20117-4014</u>		<u>PG2059+013</u>		<u>KPD2118+3841</u>		<u>PG2223+143</u>	
53657.8384	12.15 ± 3.07	54335.1524	-12.64 ± 3.75	52188.0969	-4.91 ± 3.38	54342.1777	-2.24 ± 0.49
<u>EC20228-3628*</u>		54335.9628	-15.97 ± 3.99	<u>PG2118+126</u>		54342.1917	0.59 ± 0.49
52892.8803	-72.71 ± 5.28	54335.9803	-9.93 ± 4.04	52131.9309	-4.44 ± 2.25	54342.9286	-7.58 ± 0.42
52892.8947	-82.57 ± 4.39	54337.0496	-8.52 ± 4.41	52131.9415	-6.37 ± 2.25	54342.9427	-8.95 ± 0.47
52893.8655	-71.12 ± 2.72	54337.0671	-4.94 ± 3.86	52188.0709	3.06 ± 2.30	54343.0569	-5.47 ± 0.45
52893.8796	-73.75 ± 2.82	54338.1267	6.12 ± 3.92	52188.0780	2.04 ± 2.49	54343.0710	-5.40 ± 0.45
53301.7535	-59.81 ± 3.70	54338.1476	13.05 ± 4.61	<u>EC21373-3727</u>		<u>PG2226+094</u>	
53301.7678	-53.74 ± 3.70	54338.9547	-15.85 ± 2.94	53659.7701	34.66 ± 3.59	52183.1058	-41.45 ± 3.17
53547.0925	-43.94 ± 12.62	54338.9757	-9.39 ± 3.02	53659.7811	42.20 ± 3.92	52183.1164	-40.02 ± 3.27
53547.1070	-64.40 ± 9.48	54340.0747	-13.31 ± 3.38	53664.8178	38.89 ± 2.97	<u>EC22464-6822*</u>	
53548.9771	-31.17 ± 6.03	54340.0957	-4.47 ± 3.56	53664.8285	43.74 ± 2.95	53656.9400	-10.13 ± 8.05
53548.9913	-39.32 ± 6.07	54343.0146	-7.59 ± 4.10	53665.8739	39.84 ± 3.39	53656.9474	-17.03 ± 8.09
53655.8592	-59.08 ± 6.34	54343.0321	-13.71 ± 4.42	53665.8849	37.55 ± 3.62	53657.8825	9.54 ± 7.31
53655.8771	-57.56 ± 5.24	<u>EC21043-4017*</u>		<u>PG2148+095</u>		53657.8897	6.53 ± 7.26
53657.7735	-41.37 ± 20.19	53659.7417	-6.71 ± 6.61	52182.0606	-146.23 ± 2.37	53658.9104	-6.27 ± 13.97
53657.7959	-74.04 ± 16.57	53659.7514	-30.37 ± 5.55	52182.0642	-151.44 ± 2.33	53658.9177	17.73 ± 12.91
53658.7805	-74.64 ± 5.00	53659.8710	-13.20 ± 9.22	52183.0784	-131.90 ± 2.55	53661.9964	42.43 ± 24.46
53658.7947	-69.79 ± 4.39	53659.8817	-3.16 ± 22.34	52183.0820	-143.71 ± 2.66	53664.9629	-17.27 ± 3.93
53662.7387	-69.88 ± 7.47	53663.8961	-11.58 ± 4.83	52186.0735	-133.83 ± 4.25	53664.9701	-20.53 ± 4.07
53663.8274	-75.33 ± 4.50	53664.7376	-37.49 ± 4.23	52186.0771	-142.78 ± 4.09	53665.8498	7.56 ± 5.69
53663.8461	-74.55 ± 4.10	53664.7486	-20.42 ± 3.95	<u>EC21494-7018</u>		53665.8572	24.90 ± 5.81
<u>EC20229-3716*</u>		<u>EC21079-3548</u>		53658.9331	45.47 ± 16.42	53665.9819	-21.44 ± 8.62
52892.8565	-15.27 ± 2.14	53664.7683	-94.18 ± 10.42	53658.9376	29.70 ± 6.84	53665.9892	-21.59 ± 6.99
52892.8643	-15.92 ± 4.07	53664.7837	-90.67 ± 5.01	53658.9422	47.99 ± 19.22	<u>KPD2254+5444</u>	
52893.8437	-8.07 ± 1.70	53664.7988	-87.66 ± 5.28	53659.7931	28.93 ± 4.20	52183.1492	-2.37 ± 4.26
52893.8509	-6.38 ± 1.68	53666.7834	-82.74 ± 4.17	53659.7969	42.64 ± 5.93	52183.1598	-16.79 ± 4.31
52896.7589	-12.55 ± 1.89	53666.7989	-74.84 ± 4.61	53661.9779	34.54 ± 4.92	52186.1375	-14.60 ± 5.88
52896.7661	-12.77 ± 1.97	53667.7943	-78.00 ± 8.16	53661.9817	46.37 ± 5.21	52186.1481	-19.91 ± 6.54
53109.1553	-16.17 ± 2.09	53667.8089	-79.94 ± 8.84	<u>PG2205+023</u>		52187.1132	-21.91 ± 4.56
53109.1625	-13.40 ± 2.12	<u>KPD2109+4401</u>		52182.0729	-11.92 ± 5.08	52187.1238	-29.19 ± 4.37
53547.1272	-15.72 ± 2.44	52129.9771	-40.85 ± 2.08	52182.0765	-10.63 ± 5.08	54336.0858	-7.85 ± 3.20
<u>EC20387-1716</u>		52129.9911	-38.70 ± 2.07	52183.0904	-2.38 ± 6.13	54336.1067	-9.46 ± 3.26
52895.8730	-76.20 ± 20.19	52130.1569	-34.51 ± 2.30	52183.0940	-0.67 ± 6.14	54336.9583	-15.57 ± 3.33
52896.8160	-63.94 ± 3.92	52130.1709	-33.49 ± 2.32	52186.0854	-7.80 ± 9.96	54336.9792	-4.31 ± 3.15
52896.8301	-61.39 ± 3.75	52131.0000	-32.55 ± 11.54	52186.0890	0.07 ± 10.34	54339.1834	-18.76 ± 3.17
52897.7926	-58.30 ± 3.20	52131.0140	-37.94 ± 4.52	<u>EC22081-1916</u>		54339.2009	-18.49 ± 3.13
52897.8068	-59.23 ± 2.99	52180.0671	-29.11 ± 2.93	53654.9486	-21.77 ± 19.01	<u>EC22550-1351</u>	
53302.7962	-25.33 ± 13.16	52180.0844	-35.35 ± 2.99	53655.9599	3.41 ± 12.09	53664.8990	-32.38 ± 6.30
53302.8119	-54.11 ± 4.11	52180.0984	-24.39 ± 2.76	53655.9671	-9.01 ± 11.72	53664.9132	-26.21 ± 6.29
53549.1262	-52.66 ± 6.23	<u>PG2110+127</u>		53664.8741	-24.90 ± 5.93	<u>EC22591-7129</u>	
53549.1404	-49.84 ± 6.73	52182.0317	31.83 ± 1.41	53664.8814	-37.10 ± 5.81	53300.8998	47.34 ± 6.49
<u>KPD2053+5632</u>		52182.0423	34.22 ± 1.44	53666.8519	-19.17 ± 9.62	53300.9140	49.94 ± 6.46
52188.9010	-4.04 ± 3.46	52187.0613	23.89 ± 1.88	53666.8591	-34.08 ± 10.47	53301.9085	37.49 ± 7.81
52188.9115	-3.72 ± 3.30	52187.0683	22.54 ± 1.99	<u>EC22133-6446</u>		53301.9227	40.55 ± 6.56
52393.2000	10.33 ± 4.85	52188.0466	27.29 ± 1.37	53664.9317	-5.88 ± 9.04	53302.9493	45.73 ± 8.04
52393.2142	2.46 ± 4.21	52188.0572	27.85 ± 1.39	53664.9461	-29.80 ± 8.47	53302.9635	43.37 ± 7.54
<u>PG2059+013</u>		52188.9283	16.46 ± 1.68	53665.9603	0.14 ± 14.10	53545.1578	29.14 ± 14.63
52128.9760	9.15 ± 8.28	52188.9388	15.17 ± 1.66	53667.9026	18.41 ± 25.46	53545.1730	32.60 ± 15.56
52128.9866	-12.43 ± 12.03	54331.0396	29.58 ± 1.88	<u>EC22143-6122</u>		<u>EC23073-6905</u>	
52182.0006	11.62 ± 4.29	54331.0536	25.51 ± 1.44	53666.8745	49.52 ± 6.76	52896.9821	22.70 ± 4.19
52182.0146	7.70 ± 4.51	54331.9293	27.61 ± 1.24	53666.8887	52.28 ± 7.01	52896.9928	26.69 ± 3.81
52188.0155	-0.75 ± 4.19	54331.9433	28.27 ± 1.13	<u>PG2223+143</u>		52898.0215	31.99 ± 6.50
52188.0295	1.53 ± 4.61	54334.1127	25.09 ± 1.10	54340.0227	-4.32 ± 0.39	52898.0322	39.71 ± 7.88
52188.8698	-18.00 ± 6.47	54334.1268	26.15 ± 1.11	54340.0436	-1.81 ± 0.41	53300.8697	38.53 ± 6.14
52188.8839	-2.30 ± 5.60	54335.0612	24.39 ± 1.14	54341.0172	-6.87 ± 0.43	53300.8804	38.21 ± 5.74
54330.0954	3.21 ± 3.13	54335.0753	25.07 ± 1.14	54341.0347	-6.14 ± 0.42	53545.1915	28.32 ± 13.72
54330.1129	-4.54 ± 3.11	54337.0107	25.06 ± 1.23	54341.0976	-1.40 ± 0.55	53545.2024	35.04 ± 15.39
54332.1062	-5.07 ± 4.75	54337.0247	25.82 ± 1.23	54341.1151	0.78 ± 0.54	<u>PG2314+076*</u>	
54332.1237	-2.34 ± 6.51	54342.8876	25.87 ± 1.01	54341.9111	-3.20 ± 0.44	52132.1551	-36.03 ± 3.10
54333.9171	-4.40 ± 3.76	54342.9051	21.36 ± 0.93	54341.9286	-2.67 ± 0.43	52132.1656	-32.89 ± 3.16
54333.9346	-8.16 ± 3.91	<u>KPD2118+3841</u>		54342.0558	3.31 ± 0.45	52132.2363	-39.43 ± 3.16
54335.1314	-5.75 ± 3.41	52188.0898	-0.73 ± 3.27	54342.0733	3.18 ± 0.49	52132.2469	-39.15 ± 3.69

Table 10. Previously unpublished radial velocities for the remaining sdBs in our survey. Some of these show no significant variation. Others (which we mark with an asterisk) show signs of orbital variations but our data is insufficient to distinguish between competing aliases.

HMJD	RV (km s ⁻¹)	HMJD	RV (km s ⁻¹)	HMJD	RV (km s ⁻¹)	HMJD	RV (km s ⁻¹)
<u>PG2314+076*</u>		<u>PG2314+076*</u>		<u>PG2317+046*</u>		<u>EC23483-6445</u>	
52133.0195	-31.33 ± 2.54	54341.1389	-39.29 ± 2.20	52182.1409	-42.77 ± 2.00	53301.9581	13.18 ± 4.65
52133.0335	-31.14 ± 2.50	54341.1599	-38.16 ± 1.92	52182.1549	-41.03 ± 2.18	53303.0139	20.51 ± 6.85
52180.1209	-32.30 ± 2.98	<u>PG2317+046*</u>		52184.0756	-75.94 ± 12.40	53303.0280	10.26 ± 7.28
52180.1334	-23.46 ± 3.35	52128.0886	-85.62 ± 7.24	52184.0896	-66.75 ± 4.12	53546.1780	15.15 ± 3.68
52181.1089	-45.07 ± 4.79	52128.0911	-108.52 ± 7.53	52186.0248	-43.18 ± 4.25	53546.1921	19.89 ± 4.41
52181.1229	-35.20 ± 11.44	52129.1416	-88.57 ± 6.60	52186.0537	-42.05 ± 4.11	<u>PG2349+002</u>	
52182.1084	-26.60 ± 1.99	52129.1451	-80.81 ± 6.84	54330.1793	-76.56 ± 2.04	52131.0276	30.85 ± 4.91
52182.1224	-26.23 ± 2.05	52130.1864	-93.06 ± 4.47	54330.1933	-73.87 ± 2.05	52131.0312	28.45 ± 4.88
54331.0833	-47.11 ± 2.19	52130.1935	-80.06 ± 4.55	54333.0883	-66.06 ± 2.69	52131.2213	25.28 ± 3.03
54331.0974	-46.17 ± 2.18	52131.1697	-106.50 ± 3.99	54333.1023	-61.30 ± 2.54	52131.2284	27.27 ± 3.12
54335.0969	-42.03 ± 1.81	52131.1768	-103.76 ± 3.99	<u>EC23483-6445</u>		52132.2000	36.52 ± 2.90
54335.1110	-51.06 ± 1.79	52133.1058	-99.45 ± 2.43	53300.9640	7.39 ± 4.29	52132.2071	41.75 ± 2.88
54337.0951	-39.74 ± 2.33	52133.1198	-95.54 ± 2.50	53300.9782	8.42 ± 4.33	52132.2565	48.75 ± 7.32
54337.1092	-42.97 ± 2.25	52181.1417	-39.79 ± 7.44	53301.9440	19.21 ± 4.46	52132.2601	30.17 ± 11.72